RSC Advances

ROYAL SOCIETY OF CHEMISTRY

www.rsc.org/advances

Journal Name

RSC Advances Accepted Manuscript

ARTICLE

Chemistry and Biology of microsomal Prostaglandin E$_2$ Synthase-1 (mPGES-1) Inhibitors as Novel Anti-inflammatory Agents: Recent Developments and Current Status

Puneet Khurana and Sanjay M. Jachak*

Prostaglandin (PG) E$_2$, a key mediator of inflammatory pain and fever is biosynthesized from PGH$_2$ by microsomal prostaglandin E$_2$ synthase-1(mPGES-1). During inflammation the expression of mPGES-1 increases resulting in increased PGE$_2$ formation. Specific inhibition of mPGES-1 reduces the biosynthesis of PGE$_2$ sparing other physiologically important PGs such as prostacyclin (PGI$_2$) and thromboxane A$_2$ (TXA$_2$). Inhibition of mPGES-1 might be superior over the inhibition of cyclooxygenases (COX) as the later leads to the suppression of PGI$_2$, TXA$_2$ along with the pathogenic PGE$_2$ resulting in gastro-intestinal, renal and cardiovascular complications. Therefore, inhibition of mPGES-1 has been proposed as a promising approach for the development of drugs for inflammation and pain therapy, which only suppresses PGE$_2$ biosynthesis, avoiding the side effects caused by Nonsteroidal Anti-inflammatory drugs (NSAIDs) and specific COX-2 inhibitors. The proposed review article includes natural and synthetic inhibitors of mPGES-1 reported since 2000 with their in vitro activity (IC$_{50}$ values), in vivo activity, the status of clinical candidates, and critical appraisal of these reported inhibitors.

Introduction

Inflammation is defined as an immediate response of the body to injuries of vascularized tissues that delivers blood cells and fluid at the site of damage[1]. It is the body's way of dealing with infections and tissue damage, but if the balance between the beneficial effects of inflammation and tissue destruction is not maintained, it can lead to the development of diseases such as chronic asthma, rheumatoid arthritis (RA), multiple sclerosis, inflammatory bowel disease, psoriasis, and cancer[2]. Inflammation is biochemically induced by a group of physiologically active lipid compounds known as prostaglandins that induce hormone-like effects in animals[3]. PGE$_2$ is the most abundant prostaglandin in humans and besides, having a number of physiological actions, is the key mediator of inflammation, pain, and fever[4,5]. PGE$_2$ induces its various physiological actions through binding with specific G-protein coupled Prostaglandin E$_2$ (EP) receptor subtypes EP$_1$-EP$_4$ located on the cell surface[6].

Various studies showed increased levels of PGE$_2$ in the synovial fluid of patients with RA and osteoarthritis (OA)[7,8]. Thus, two approaches associated with the reduction of pain and inflammation in various diseases can be either decreasing the biosynthesis of PGE$_2$ or obstructing the binding of PGE$_2$ to its EP receptors. In the present review, we will be focusing on the former approach.

Elevated levels of COX-2 and concomitant overproduction of PGE$_2$ have been shown to be associated with all inflammatory diseases and various types of cancers[9]. These observations led to the use of NSAIDs and specific COX-2 inhibitors as the first line drugs for the treatment of inflammation, pain, and swelling in RA and OA. But the prolonged use of non-specific COX inhibitors led to gastrointestinal side effects. To overcome these frequently observed gastro-intestinal side effects of NSAIDs, second generation COX-2 selective inhibitors (coxibs) were developed. Unfortunately, the COX-2 selective NSAIDs were linked to increased risk of myocardial infarction and renal toxicity[10]. Subsequently, it was believed that inhibition of COX enzymes led to the suppression of the biosynthesis of physiologically important PGs such as prostacyclin (PGI$_2$), and thromboxane A$_2$ (TXA$_2$) along with the pathogenic PGE$_2$ resulting in gastro-intestinal, renal and cardiovascular complications[11]. Therefore, selective inhibition of PGE$_2$ biosynthesis was hypothesized to provide regulation of inflammation, with improved safety profile compared to the NSAIDs or coxibs.

Department of Natural Products, National Institute of Pharmaceutical Education and Research (NIPER), Sector-67, SAS Nagar, (Mohali)-160062, Punjab, India.
E-mail: sanjayjachak@niper.ac.in; Fax: +91 172 2214692; Tel: +91 172 2214683
* Corresponding Author

A concerted action of COXs and PGE_2 synthases (PGES) catalyze the biosynthesis of PGE_2 from arachidonic acid (AA). PGES is the enzyme involved in the terminal step of the biosynthesis of PGE_2, which catalyzes the conversion of COX-derived PGH_2 to PGE_2 (Figure **1**). Different terminal isoforms of PGES have been identified: cytosolic PGES (cPGES), membrane PGES-1 (mPGES-1) and membrane PGES-2 (mPGES-2), and a preferential functional coupling between COX and PGES isoenzymes have been shown by co-expression studies. Both cPGES and mPGES-2 are constitutively expressed enzymes and primarily provide PGE_2 for homeostasis, in which cPGES is coupled to COX-1 and mPGES-2 is coupled to both COX-1 and COX-2. The mPGES-1 enzyme is coupled to COX-2 and represents the only isoform induced by various inflammatory stimuli, such as interleukin-1-β (IL-1β)[12,13]. Thus, mPGES-1 appears to be a better target for discovery and development of new anti-inflammatory drugs.

1. mPGES-1

mPGES-1 belongs to the family of Membrane-Associated Proteins in Eicosanoid and Glutathione metabolism (MAPEG), possessing highly divergent functions. The other enzymes of MAPEG family are leukotriene C_4 (LTC_4) synthase, 5-lipoxygenase-activating protein and microsomal glutathione S-transferases (MGSTs)[14]. Structurally, mPGES-1 shares 39% sequence identity with MGST-1. Human mPGES-1 is a membrane protein of 15-16 kDa and it is the first isoform of PGES identified and cloned by Jakobsson et al. in 1999 as an inducible and glutathione-dependent enzyme[15]. In 2008, a 3D-electron crystallography structure of mPGES-1 was reported but the detailed analysis of the protein organization suggested a closed non-active form[16]. In 2013, first high-resolution X-ray structure of mPGES-1 was introduced in the active form that enabled more efficient and accurate structure-based design of new potent inhibitors (PDB code: 4AL0)[17]. mPGES-1 is a homotrimer (chain A, B, and C) consisting of 152 amino acids, with each monomer consisting of four trans membrane helices (TM1-4) and a large cytoplasmic loop between TM1 and TM2 (Figure **2A**). The three TM2s of each trimer form an inner core with a funnel-shaped opening towards the cytoplasmic side. Glutathione (GSH) is an essential cofactor for its catalytic turnover. It binds at the interface between subunits in the protein trimer exposed to the lipid bilayer in U-shaped conformation mainly via hydrogen bonds involving the side chains of Arg73, Asn74, Glu77, His113, Tyr117, Arg126, and Ser127 from helices II and IV and the side chain of Arg38 from helix I (Figure **2C**). The enzyme undergoes conformational changes from a closed to an open conformation before PGH_2 can access the active site[18,19]. Thus, in a structure-based design, a hypothetical inhibitor can act either as a false substrate (PGH_2) or as a cofactor analog (GSH) or can behave in both the ways. The key interactions an inhibitor must possess with the receptor counterpart are following:

- π-π interaction with Tyr130(A), indicative of a good accommodation within the GSH binding site

- a polar interaction with Ser127(A), a key residue involved in PGH_2 recognition
- polar interactions with Thr131(A), Gln134(A), and Vander Waals interactions with Tyr28(B) and Ile32(B), belonging to the external binding groove[20].

To study the mechanism of action of mPGES-1, a catalytic process has been proposed in which GSH covalently binds PGH_2 that subsequently isomerizes to PGE_2 (Figure **3**). Ser127 activates the thiol of GSH to form a thiolate anion that exerts a nucleophilic attack on the endoperoxide oxygen atom at the C-9 carbon of PGH_2 to produce an unstable reaction intermediate (2). The subsequent proton abstraction at C-9 followed by S·O bond cleavage is mediated by Asp49 that forms a bidentate complex with Arg126. (3) This results in the regeneration of the reactive thiolate anion and the formation of the product PGE_2[17].

2. mPGES-1 as a pharmacological target

mPGES-1 is constitutively expressed in very low quantities in almost every tissue but its expression remarkably increases in response to an inflammatory stimuli[21]. mPGES-1 receives its substrate PGH_2 derived from COX-2 and forms PGE_2, the main mediator for carrying out the inflammatory response. Besides, being a mediator for inflammation, PGE_2 possesses multiple physiological functions like synaptic transmission via EP_2 receptors[22], renal sodium and water transportation[23] and regulation of female reproductive functions in ovulation, embryo implantation, and formation of corpus luteum[24]. mPGES-1 is emerging as a promising drug target for inflammatory diseases because its inhibition leads to the reduction of inducible PGE_2 by mechanisms that overcome the toxicity associated with the inhibition of COX-1 and COX-2. mPGES-1 is over-expressed and plays an important role in diseases related to inflammation and cancer. Increased levels of PGE_2 have been detected in serum and synovial fluids of the patients suffering from RA and OA[25-27], in intestinal mucosa of patients with inflammatory bowel diseases[26]and in the heart tissue after myocardial infarction[28,29]. It is also abundant in liver tissue and muscles of patients with hepatitis and polymyositis respectively[30,31]. Recently it is reported that mPGES-1 is involved in the pathogenesis of different cancers and in the induction of angiogenesis. mPGES-1 is overexpressed in gastrointestinal (GI) cancers including esophageal[32], gastric[33-36], colorectal[37,38], liver[39,40] and pancreatic cancers[41], brain cancers (gliomas and medulloblastomas[42,43]), breast cancer[44],kidney cancer[45], thyroid cancer[46] and several cancers derived from the epithelium (including head and neck[47,48], penis[49], lungs[50-52], larynx[53], cervix[54], endometrium[55] and ovary[56]). PGE_2 also plays a significant role in various neurological diseases like Alzheimer's disease (AD), amyotrophic lateral sclerosis, Creutzfeldt–Jakob disease, ischemic stroke, and HIV-associated dementia[57]. Thus, mPGES-1 inhibition could be considered as a valid strategy for the treatments of inflammatory diseases. It was reported that mice deficient in mPGES-1 were protected

from fever, and chronic inflammation, and were not predisposed to thrombogenesis or hypertension[58].

3. mPGES-1 inhibition assays

The basic principle of all the mPGES-1 inhibitory assay procedures lies in the quantitative determination of PGE_2 formed by the catalytic action of mPGES-1 on its substrate PGH_2. Short reaction time and low temperature are the prime requirements of the assay procedure due to instability PGH_2 that rapidly converts to PGD_2 and PGE_2 with a $t_{1/2}$ of 10 min at pH 7 and 20°C[59]. There are different reported methods for the quantitative measurement of PGE_2 formed from PGH_2. They include Reverse Phase High Performance Liquid Chromatography (RP-HPLC), Enzyme-Linked Immunosorbent Assay (ELISA)-based method, and Homogenous Time Resolved Fluorescence (HTRF)-based method. In the RP-HPLC method, 11-β-PGE_2 is used as an internal standard and PGE_2 is analyzed by an HPLC method on a C-18 column with a mobile phase comprising of water, acetonitrile, trifluoroacetic acid; 72:28:0.007, detected at 195 nm[60]. There are special commercially available analytical kits for ELISA and HRTF based methods for the quantitative determination of PGE_2.

3.1 Expression and purification of mPGES-1

There are many reported cell lines in which mPGES-1 can be expressed like A549, *E.coli*, HeLa, HEK293, RAW 264.7 (murine macrophages), *Pichia pastoris* (KM71H strain), and Sf9 insect cells[12,54,61]. After the expression of mPGES-1 in any of the above cells, the microsomal fraction containing the enzyme is isolated from the cells.

3.1.1 Induction of mPGES-1 in A549 cells and isolation of microsomes

Preparation of A549 cells and the procedure of isolation of its microsomes was firstly reported by Jakobsson *et al.* in 1999[15]. In brief, cells (2×10^6 cells in 20 ml of medium) were plated in 175-cm^2 flasks and incubated for 16 h at 37°C and 5% CO_2. Subsequently, the culture medium was replaced by fresh Dulbecco's Modified Eagle's Medium (DMEM)/high glucose (4.5 g/l) medium containing fetal calf serum [2% (v/v)]. To induce mPGES-1 expression, 1 ng/ml IL- 1β was added, and the cells were incubated for another 72 h. Thereafter, the cells were detached with 1×trypsin/ Ethylenediamine tetraacetate (EDTA), washed with phosphate buffer saline (PBS), and frozen in liquid nitrogen. Ice-cold homogenization buffer (0.1 M potassium phosphate buffer pH 7.4, 1 mM phenylmethylsulfonyl fluoride (PMSF), 60 μg/ml soybean trypsin inhibitor, 1 μg/ml leupeptin, 2.5 mM GSH, and 250 mM sucrose) was added; after 15 min, cells were resuspended and sonicated on ice (3 × 20 s). The homogenate was subjected to differential centrifugation at 10,000 g for 10 min and at 174,000 g for 1 h at 4°C. The pellet (microsomal fraction) was resuspended in 1 ml of homogenization buffer, and the protein concentration was determined by the Coomassie protein assay[60].

3.1.2 mPGES-1 expression in Sf9 cells and purification

The human mPGES-1 (GenBank accession no. BC008280) was PCR-cloned from a placenta cDNA library. The coding sequence of mPGES-1 was inserted into a baculovirus DNA using direct baculovirus expression system. The recombinant virus was amplified and used to infect Sf9 cells cultivated in Sf-900 media with a multiplicity-of-titer of 2 at a cell density of 3×10^6 cells/mL. mPGES-1 was purified according to Ouellet *et al.*[62,63]. Briefly, cells were harvested 70 h post infection by centrifugation and resuspended in 15 mM Tris·HCl pH 8, 0.25 M Sucrose, 0.1 mM EDTA, and 1 mM reduced L-GSH. After disruption of the cells, a microsomal fraction was prepared by ultracentrifugation and the mPGES-1 was solubilized from the membranes by addition of 3% (wt/vol) β-octylglucoside in 10 mM potassium phosphate pH 7, 10% (wt/vol) glycerol, 0.1 mM EDTA, and 1 mM GSH. The solubilized enzyme was finally purified on hydroxylapatite (Macroprep ceramic hydroxylapatite type 1)[64].

3.1.3 mPGES-1 expression in *E.coli* and purification

The coding regions of human mPGES-1 in pPGES or pPGES-mut were expressed in various strains of *E. coli*, such as BL21 (DE3), Rosetta (DE3), and Rosetta (DE3)/pRARE. To obtain pure mPGES-1, Rosetta (DE3) cells harboring pPGES-mut were grown at 37° C in LB medium containing 30 μg/ml kanamycin and 34 μg/μl chloramphenicol until the optical density (OD)$_{600}$ of the culture reached 0.5-0.7. mPGES-1 expression was induced by addition of isopropyl β-D-1-thiogalactopyranoside (IPTG) to 1 mM final concentration, further growth for 12 h at 18° C, and the cells harvested by centrifugation (5,000 g, 20 min) at 4° C. The cell pellet was suspended in 5 volumes of lysis buffer (15 mM Tris-HCl, pH 7.4, 0.25 M sucrose, 1 mM EDTA, 1 mM PMSF, and 1 mM GSH), lysed by ultrasonication, and removed by centrifugation (5,000 g, 10 min) at 4° C. The membrane fraction in the supernatant was precipitated by ultracentrifugation (100,000 g, 1 h) at 4° C, resuspended in 20 ml of solubilization buffer (15 mM Tris-HCl, pH 7.4, 150 mM NaCl, 10% glycerol, 0.5 mM EDTA, 1 mM PMSF, 1 mM GSH, and 4% Triton X-100) for 3 h on ice with stirring, and the insoluble material removed by ultracentrifugation (100,000 g, 30 min) at 4° C. The supernatant was next loaded onto a Ni-NTA chromatography column equilibrated with buffer A (15 mM Tris-HCl, pH 7.4, 150 mM NaCl, 10% glycerol, and 0.2% Triton X-100), washed with buffer A and then washing buffer (50 mM imidazole in buffer A), and the bound protein eluted with elution buffer (200 mM imidazole in buffer A) and immediately loaded onto a mono Q-sepharose column[65].

3.1.4 Cell-Free Expression of Human mPGES-1

Human mPGES-1was obtained by the continuous-exchange cell-free expression system according to Schwarz *et al.* (2007). This system comprises a reaction mixture (RM) that contains the *Escherichia coli* S30 extract (derived from the A19 strain), T7 polymerase, tRNAs, pyruvate kinase, and the template DNA for human mPGES-1 (cloned in the pBH4 vector derived from pET19b; Novagen, Madison, WI). The RM is dialyzed against

the feeding mixture that supplies amino acids, energy equivalents acetyl phosphate and phosphoenol pyruvate, and nucleotides. Reactions were incubated at 30°C for up to 20 h. Protein synthesis takes place in the RM and up to 1.5 mg of mPGES-1/ml RM can be obtained. mPGES-1 was resuspended in 50 mM potassium phosphate buffer, pH 7.4, 1 mM glutathione, 10% glycerol, and 2% (w/v)1-lauroyl-2-hydroxy-*sn*-glycero-3-phosphocholine (LysoFos12 choline; Anatrace, Maumee, OH) for 2 h at 30°C, and insoluble parts were removed by centrifugation (10,000 g, 10 min, 10°C)[66].

3.2 mPGES-1 inhibitory assay procedure

3.2.1 Cell-free assay

Required amount of protein of a microsomal preparation expressed by any of the above-mentioned methods was incubated with a known concentration of the sample or the vehicle (DMSO) for 15 minutes at 4°C in phosphate buffer (0.1 M, pH 7.4) containing 2.5 mM glutathione. The reaction was initiated by addition of a standardized amount of PGH_2. After 1 min at 4°C, the reaction was terminated using stop solution (40 mM $FeCl_2$, 80 mM citric acid). PGE_2 formed by the reaction was quantitatively determined by either RP-HPLC method[60], ELISA based method[67], or by HTRF based method[68]. The% control activity was calculated as the percentage difference between negative control (100% inhibited with a reference compound) and enzyme only control. The difference between enzymatic versus non-enzymatic production of PGE_2 is typically 3-4 fold. IC_{50} values were calculated by a 4 parameter log fit of the % control data. These parameters are minimum asymptote, slope, inflection point, and maximum asymptote.

3.2.2 Cell-based assay

Determination of PGE_2 Formation in Intact RAW 264.7Cells

Expression of mPGES-1 in RAW 264.7 cells was induced by incubation with lipopolysaccharide (1 µg/ml) for 20 h. Cells were washed twice with PBS, resuspended in PBS (10^6/ml), and preincubated with the indicated compounds at 37°C for 10 min. PGE_2 formation was started by the addition of AA (1 µM). The reaction was stopped after 15 min at 37°C, and the samples were put on ice. For quantification of PGE_2, samples were extracted, fractionated by HPLC, and then quantified using a PGE_2 High Sensitivity EIA Kit[69].

Determination of PGE_2 formation in intact A549 cells

IL-1β-treated A549 cells, cultured in PBS containing $CaCl_2$ (1 mM) were pre-incubated with test compounds or vehicle (DMSO, never exceeding a final concentration of 0.3%) at 37°C for 10 min, and PGE_2 formation was started by the addition of ionophore A23187 (5-methylamino-2-[[(2S,3R,5R,8S,9S)-3,5,9-trimethyl-2-[(2S)-1-oxo-1-(1H-pyrrol-2-yl)-propan-2-yl]-1,7 dioxaspiro[5.5]undecan-8-yl]methyl]-1,3-benzooxazole-4-carboxylic acid, 2.5 µM), AA (1 µM), and [^{3}H]AA(18.4 kBq). The reaction was stopped after 15 min on ice. After centrifugation (800 g, 5 min, 4°C), the supernatant was acidified (pH 3) by the addition of citric acid (20 µl, 2 M), and the internal standard

11β-PGE_2 (2 nM) was added. Radiolabeled PGE_2 was separated by RP-18 solid phase extraction and HPLC. The amount of 11β-PGE_2 was quantified by integration of the area under the eluted peaks. For quantification of radiolabeled PGE_2, fractions (0.5 ml) were collected and mixed with Ultima GoldTM XR (2 ml) for liquid scintillation counting in an LKB Wallac 1209 Rackbeta Liquid Scintillation Counter[70].

Determination of PGE_2 formation in human fetal fibroblasts

Human fetal fibroblasts (FF), plated at 3×10^6 cells/cm^2 in DMEM, supplemented with 15% fetal bovine serum (FBS), glutamine, penicillin/streptomycin and (4-(2-hydroxyethyl)-1-piperazineethanesulfonic acid (HEPES), were incubated at 37°C, 5% CO_2. Approximately 20–24 h later, media were refreshed and cells were treated with 1 ng/mL IL-1β for an additional 20–24 h, after which they were washed once with DMEM without serum. Cells were then incubated with compounds for 50 min in DMEM without serum and then with 10 µM AA for 10 min. PGE_2 levels were analyzed by ELISA[71].

3.2.3 LPS-stimulated human whole blood assay (LPS/HWB)

Human whole blood was collected in 10 ml heparinized tubes from healthy human donors who had not taken NSAIDS or COXibs for the preceding 5 days. Blood was stimulated with 20 µg/ml LPS for 24 h in the presence of vehicle (1% DMSO) or the inhibitors (1% DMSO), at 37° C in 95% air, 5% CO_2 atmosphere. The assay plates were centrifuged at 930×g for 10 min at room temperature and the plasma was removed for the quantitation of PGE_2 levels by ELISA[72].

3.3 Identifying molecules that inhibit expression of mPGES-1

It is an alternative method for inhibiting inducible PGE_2 synthesis by attenuating the transcriptional activation of mPGES-1. A cell-based screening system, using luciferase activity as readout, has been developed to identify selective down-regulators of mPGES-1 expression[73].

4. mPGES-1 inhibitors

A number of compounds of natural as well as synthetic origin have been reported as mPGES-1 inhibitors. The aim of the proposed review is to cover the recent developments of the new compounds as mPGES-1 inhibitors from natural products and of synthetic origin. The review covers 191 mPGES-1 inhibitors of natural product and synthetic origin, studied till date with their activity profile along with Standard Error of Mean (SEM), wherever available. These compounds are classified into the following classes:

- Synthetic mPGES-1 inhibitors
- Natural product compounds as mPGES-1 inhibitors

4.1 Synthetic small molecules as mPGES-1 inhibitors

Extensive work has been done for identification and characterization of synthetic molecules as mPGES-1 inhibitors. We have provided classification of synthetic mPGES-1 inhibitors based on the chemical scaffold used to synthesize these molecules:

1. Arylpyrrolizines
2. Biarylimidazoles
3. MK-886 derivatives
4. Benzo[g]indol-3-carboxylate derivatives
5. Benzoxazole derivatives
6. Phenanthrene imidazole derivatives.
7. Imidazoquinolines
8. Oxicam Derivatives
9. Pyrrole alkanoic acid derivatives
10. Trisubstituted urea derivatives
11. Pirnixic acid derivatives
12. 2-Mercaptohexanoic acid derivatives
13. Quinazolin-4(3H)-one derivatives
14. Carbazole benzamide derivatives
15. 1,2,3-triazole derivatives
16. Endogenous fats, lipids and PGH_2 analogs
17. Anti-inflammatory drugs
18. Miscellaneous inhibitors

4.1.1 Arylpyrrolizines

Arylpyrrolizines are well-recognized scaffolds as dual COX/LOX inhibitors and this class of compounds was recently reported to exhibit mPGES-1 inhibitory activity as well[60]. Several arylpyrrolizine derivatives (Table **1**) were prepared based on the lead structure of licofelone (**1**) (IC_{50} = 6.7 μM) that was modified at the acid group. The aim is to optimize the mPGES-1 inhibition potency of these molecules, reducing or abolishing COX activity and at the same time retaining 5-LOX inhibitory activity. Substitution of the *p*-chloro atom of the phenyl ring of licofelone by NO_2, CF_3 or *tert*-butyl resulted in significant decrease in potency against mPGES-1 (IC_{50}> 10 μM). Replacement of acetic acid group in position C-5 of licofelone by propionic acid group resulted in chemically more stable molecules. Substitution of tolyl sulfonimides at free acid functionality resulted in compound **(2)** that was 1.4 times potent than licofelone (IC_{50} = 4.8 μM). Comparable results were observed by substitution of tolyl group by a simple phenyl group (IC_{50} = 4.5 μM). The derivative **(3)** with tolyl sulfonamide substitution at the acid functionality and propionic acid group at C-5 was 3-fold superior to licofelone in the mPGES-1 assay and equipotent to MK-886 (IC_{50} = 2.1 μM). Replacement of carboxylic acid of licofelone with a tetrazole moiety resulted in the molecule **(4)** with similar potency as that of aryl sulfonimides (IC_{50} = 3.9 μM)[74].

4.1.2 Biarylimidazoles

A number of biarylimidazole derivatives demonstrated potent mPGES-1 inhibitory activity with IC_{50} values in the range of 0.001 μM. The SAR studies were performed at four positions of the biarylimidazole scaffold: the 2nd, 4th and 5th position and at the central imidazole ring. Bis-*ortho*-chlorofluoro substitution pattern at the 2nd position, **(5)** (Table **2**) showed the maximum affinity for the mPGES-1 enzyme (IC_{50} = 0.66 μM). Changing the position of nitrogen atom in the imidazole ring resulted in reduced activity against mPGES-1. Replacement of the imidazole ring with oxadiazole ring led to complete loss in activity whereas a triazole ring resulted in more potent

derivatives. SAR carried out at the 4th position of the imidazole skeleton revealed that hydrophobic groups result in potent derivatives. Alkyne linkage in compound **(6),** is superior over alkene and alkane linkage (IC_{50} = 0.008 μM). Introducing pyridine ring resulted in compound **(7)** and **(8)** with similar potencies with IC_{50} of 0.023 μM, and 0.013 μM respectively. Introduction of an electron-withdrawing substituent at the 5th position resulted in most potent compounds **(9)** and **(10)** of this series with IC_{50} 0.005 μM and 0.001 μM respectively. Compound **(10)** showed an oral bioavailability of 127% and a half-life of 4.8 h in rats and an IC_{50} of 1.6 μM in the human whole blood (HWB) assay[75]. The crystal structure of mPGES-1 bound to compound **(11)** was studied with the help of crystallographic studies along with light scattering-based thermal stability assay for mPGES-1 bound to various inhibitors (Figure **4**). In the crystal structure of mPGES-1 bound to (**11**), the inhibitor was bound with the bis-*ortho*-chlorofluorophenyl inserted into a groove above GSH at the top of the pocket and formed hydrophobic and van der Waals interactions with A123 and S127 side chains (monomer 1) and R38, L39, F44, D49, H53, and R53 side chains (monomer 2). The core imidazole, in a near orthogonal orientation relative to the chlorofluorophenyl, forms hydrogen bonds with the H53 and S127 side chains and a structured water molecule (W75), and interacts hydrophobically with the P124 side chain. The bromine extends towards the solvent interacting with the side chain of R52. This orientation of the core imidazole dictates a trajectory for the pyridine, triple bond C-C linker, and trifluoromethylbenzene tail that emphasizes interactions with α-4 of monomer 1. The nitrogen of the pyridine is within hydrogen bonding distance of the side chain oxygen of T131 (monomer 1). Hydrophobic and van Waals contacts with the aforementioned "tail" functional groups are made exclusively with α-4 of monomer 1 including interactions with the P124, S127, V128, T131, L132, and L135 side chains (monomer 1)[76].

4.1.3 MK-886 derivatives

MK-886 **(12), (**Table **3)** a potent 5-lipoxygenase-activating protein (FLAP) inhibitor (FLAP IC_{50} = 0.026 μM) was also found to be a moderate inhibitor of the human mPGES-1 enzyme with an IC_{50} of 1.6 μM[77]. Using MK-886 as a lead structure, many derivatives were synthesized to discover more potent and selective mPGES-1 inhibitors. Replacement of N-*p*-chlorobenzyl substituent and the carboxylic acid group on the side chain at C_2 with other substituents resulted in a dramatic loss in potency. Introduction of a methyl group at the C_3 position of the indole led to compound **(13)** with an IC_{50} of 1 μM and was further used for SAR studies. Introducing a biphenyl moiety at C_5 of the indole dramatically increased the inhibitor potency and resulted in compounds **(14), (15),** and **(16)** with the IC_{50} values of 0.16 μM, 0.016 μM and 0.007 μM respectively. Additional *ortho* substitution with a methyl group to the biphenyl bond on the terminal phenyl group provided the most potent inhibitor in the series (**17**) with an IC_{50} of 0.003 μM. Thus, the biarylindole (**17**) was found to be 500-fold more potent inhibitor of mPGES-1 than MK-886[78]. The crystal

structure of mPGES-1 bound to **(17)** was extensively studied for its various interactions with the enzyme (Figure **5**). Compound **(17)** was bound in an elongated orientation with the long axis of the molecule parallel to the transmembrane helices which formed the pocket. The carboxylate was at the top of the binding site and formed a pair of salt bridges with the side chain of R52 (monomer 2). Bridging water was found between the **(17)** carboxylate and the H53 imidazole. In addition, an aromatic CH from the indole and another from the fluorophenyl H-bonded with the T131 hydroxyl lone pairs (monomer2). The chlorophenyl attached to the nitrogen of the indole ring extended inward between two helical turns at the top of α-4 from monomer 1 and α-1 from monomer 2 and placed the halogen on top of the glutathione sulfur. Hydrophobic van der Waals contacts were formed between the chlorophenyl and R38, L39, and F44 side chains (monomer 2) and GSH. The indole ring sat flatly across the binding site facing, but not contacting, GSH. The fluorinated biaryl extended downward from the indole with one conformation, the fluorine pointing inwards into a small groove between the Y130 and T131 side chains and in the second conformation, the fluorine pointing towards solvent. The fluorophenyl ring itself was slotted into the groove formed between the Y130 and T131 side chains (monomer 1) and was bounded on the opposite edge by the I32 side chain (monomer 2)[76].

4.1.4 Benzo[g]indol-3-carboxylate derivatives

Benzo[g]indol-3-carboxylate derivatives were discovered as dual 5-LOX/mPGES-1 inhibitors. The lead structure **(18),** (Table **4**) in this study showed a weak inhibition of mPGES-1 activity at 10µM (17 ± 8%) but was found to be a potent inhibitor of 5-LOX in cell-based (IC_{50} = 2.4 µM) and cell-free assays (IC_{50} = 0.3 µM)[79]. Potency was slightly improved by exchange of nitrogen by a methylene group (**19**) and elongation by another methylene group (**20**) at position C-2 of the indole ring. Introducing a 4-biphenyl residue at 7-position of (**19**) led to compound (**21**) with a better potency (IC_{50} = 3.1 µM). Annulation of benzene to the indole of (**18**) and (**19**) led to a more potent compounds (**22**) and (**23**) with IC_{50} values 1.6 µM and 0.6 µM respectively. Replacement of chlorine in (**23**) with fluorine, bromine, and a methoxy group yielded compounds (**24**), (**25**), and (**26**) with IC_{50} values of 0.5 µM, 0.2 µM, and 0.6 µM respectively. Substitution of chlorine in the *ortho*-position of the benzyl ring of (**23**) led to the most potent compound (**27**) of this series (IC_{50} = 0.1 µM). Compound (**23**) also showed marked inhibition of PGE_2 formation in intact (A549) cells (IC_{50} = 2 µM) and also reduced PGE_2 levels *in vivo*, showing a remarkable anti-inflammatory activity[70].

4.1.5 Benzoxazole derivatives

A series of benzoxazole mPGES-1 inhibitors was developed employing a high throughput screening of the Pfizer compound collection (Table **5**). The lead molecule (**28**) was found to be a moderate inhibitor of human mPGES-1, with an IC_{50} value of 1.2 µM. Sub-structure search of related benzoxazoles led to compound (**29**), with a better potency (IC_{50} = 0.85 µM) and selectivity for mPGES-1 over COX-2.

Modifying the piperidine and amide linker decreased the potency while changes in the amide substituent improved the potency and physical properties. The potency was moderately increased by changing the ring size of the amide substituent from five to seven membered ring (**30**) (IC_{50} = 0.82 µM). Introducing a methyl group and a phenyl ring in the 2-position of cyclopentyl ring gave more potent compounds (**31**), IC_{50} = 0.24 µM) and (**32**), IC_{50} = 0.29 µM) respectively. The potency was improved further by introducing ether groups in the cyclopentyl ring (**33**), IC_{50} = 0.82 µM) and (**34**), IC_{50} = 0.17 µM). The potency of certain derivatives depended directly on the chirality of the substituent in the cyclohexyl and cyclopentyl ring. In case of 1,4-substituted cyclohexyl derivatives, the *cis* diastereomer (**35**), IC_{50} = 0.38 µM) was more active than *trans* (**36**), IC_{50} > 19.1 µM). Similarly, in case of 1, 2-substituted cyclopentyl derivatives, the *cis* diastereomer (**37**), IC_{50} = 0.78 µM) was more active than *trans* (**38**), IC_{50} = 3.2 µM). Other 1,2-substituted cyclopentyl derivatives (**39**-**43**) with higher lipophilicity had no apparent difference in the potency between the diastereomers but were found to be the most active compounds of this series with IC_{50} of 0.043 µM, 0.034 µM, 0.082 µM, 0.04 µM, 0.018 µM respectively. Compound (**43**) inhibited PGE_2 production in the LPS/human whole blood assay with an IC_{50} = 7 µM. It exhibited 55% oral bioavailability in dogs with a half-life of 7.2 h[80].

4.1.6 Phenanthrene imidazole derivatives

MF63 (**44**), the lead molecule of this series is a potent and selective mPGES-1 inhibitor (IC_{50} = 0.001 µM)[81]. Also, it exhibited inhibition of PGE_2 in A549 cells with an IC_{50} value 0.42 µM, a human whole blood (HWB) PGE_2 inhibition activity with IC_{50} value 1.3 µM and was found active in guinea pig hyperalgesia model. The SAR studies revealed that 6th and 9th position of the phenanthrene imidazole system were critical for the bioactivity. The most potent compounds of this series were (**48**) and (**54**) with an enhanced HWB PGE_2 inhibition having IC_{50} values 0.20 µM and 0.14 µM respectively[82] (Table **6**). The crystal structure of mPGES-1 bound to (**44**) revealed that the compound (**44**) occupied the extreme upper region of the binding pocket above GSH (Figure **6**). The planar chloro-phenanthrene extended over a flat surface of α-4 of monomer 1 (P124, S127, and V128 of monomer 1), with one face of the aromatic tetracycle facing solvent. Similar to the bis-*ortho* chlorofluorophenyl of 5, a slightly larger 2,6-dicyano-phenyl pointed inwards, clamped between the two protein chains, with one nitrile on the backside directed straight forming a 3.6 A° van der Waals contact with the Cβ of A123 (monomer 1) and a 3.2 A° interaction with the side chain hydroxyl of S127 (monomer 1). The second nitrile packed against the L39 side chain (monomer 2) while engaging a network of structured waters in the front of the binding site. Carbons of the 2,6-dicyano-phenyl formed hydrophobic contacts with the sidechains of R38, L39, F44, and D49 (monomer 2), while the imidazole formed H-bonds with H53 (monomer 2)[76].

4.1.7 Imidazoquinolines

The lead molecule of this series (**55**) was found as a hit in the HTS procedure of a chemical library. Compound (**55**) showed a moderate mPGES-1 inhibitory activity (60% inhibition at 10 μM). The C-2 position of the lead molecule (**55**) seemed to be critical for the biological activity. One of the most potent compounds of this series (**56**) had an IC$_{50}$ value 0.0091 μM for mPGES-1 with high selectivity (>1000-fold) over both COX-1 and COX-2. Taking (**56**) as a new lead further SAR study on C-2 and C-7 gave (**63**), the best molecule of this series exhibiting strong mPGES-1 inhibitory activity (IC$_{50}$ = 0.0041 μM), potent cell-based functional activity (IC$_{50}$ = 0.033 μM) with good mPGES-1 selectivity (over 700-fold), excellent in vitro ADME profile, and good oral absorption in rat pharmacokinetic study. [83-85]. (Table **7**).

4.1.8 Oxicam Derivatives

Oxicam derivatives were reported as COX-1 and COX-2 inhibitors. The early lead compounds (**64**) and (**65**) of this series were discovered by HTS of the Pfizer chemical library against the human mPGES-1 having an IC$_{50}$ of 1.68 μM and 0.11 μM respectively. The most active molecule of this series (**73**) exhibited an IC$_{50}$ of 0.016 μM, displayed a remarkable PGE$_2$ inhibition in a cell-based assay (IC$_{50}$ = 0.42 μM) and a 238-fold selectivity for mPGES-1 over COX-2[71]. (Table **8**).

4.1.9 Pyrrole alkanoic acid derivatives

This class of compounds is known as nuisance inhibitors of mPGES-1 which exert their action not by directly binding to the enzyme but by sequestering and inhibiting enzyme targets by forming colloid–like aggregates at micromolar or sometimes at submicromolar concentrations. The lead compound in this series is 4-acylpyrrol-2-ylpropionic acid (**79**) which was found to reduce enzyme activity with an IC$_{50}$ of 0.80 μM[86]. (Table **9**).

4.1.10 Trisubstituted urea derivatives

The lead molecule (**87**) in this class was identified as a hit by an HTS screening program and showed 88% enzyme inhibition at 10 μM. The introduction of a rigid alkyne linker in the lead compound resulted in a remarkable increase in mPGES-1 inhibitory activity. Compound (**94**) showed maximum inhibition of mPGES-1 in the cell-free assay (IC$_{50}$ = 0.001 μM) and in A549 cell-based assay (IC$_{50}$ = 0.16 μM) but did not show activity in HWB assay. Compounds (**95**) and (**96**) showed similar potencies in cell-free and cell-based assays but due to extensive protein binding did not exhibit activity in HWB assay. Compound (**97**), the most potent molecule of this series showed an IC$_{50}$ of 0.002 μM in the cell-free assay and exhibited potent activity in A549 cell-based assay (IC$_{50}$ = 0.34 μM) and HWB assay (IC$_{50}$ = 2.1 μM)[87]. (Table **10**).

4.1.11 Pirnixic acid derivatives

Pirnixic acid (**98**) is the lead molecule of this series. Pirnixic acid derivatives were found to be dual mPGES-1 and LOX inhibitors. The biphenyl derivative (**101**) moderately inhibited mPGES-1 with an IC$_{50}$ of 1.3 μM[88]. Replacement of biphenyl group by an aminothiazole moiety revealed compound (**103**), the most potent compound of this series (IC$_{50}$ = 0.4 μM)[89]. α-(n-hexyl)

substitution at (**98**) gave a new potent molecule **YS121 (104)**, that inhibited human mPGES-1 in a reversible and noncompetitive manner (IC$_{50}$ = 3.4 μM) and exhibited a remarkable activity in HWB assay (IC$_{50}$ = 2 μM). Also, in carrageenan-induced rat pleurisy, (**104**) blocked the exudate formation and leukocyte infiltration accompanied by reduced pleural levels of PGE$_2$ and leukotriene B$_4$[69]. (Table **11**).

4.1.12 2-Mercaptohexanoic acid derivatives

This is another class of dual 5-LOX and mPGES-1 inhibitors. Compounds (**105-107**) (Figure **7**) are the most potent representatives of this series with mPGES-1 IC$_{50}$ values of 1.7, 2.2 and 2.2 μM, respectively. Compound (**107**) inhibited 5-LOX in intact cells with even a higher potency (IC$_{50}$ = 0.9 μM) and neither significantly inhibited the related 12- or 15-LOXs nor COX-1 and COX-2 or cytosolic phospholipase A$_2$[90].

4.1.13 Quinazolin-4(3H)-one derivatives

The lead compound (**108**), of this novel class of mPGES-1 inhibitors, showed 67% of enzyme inhibition at 10 μM. The SAR of this series revealed remarkably potent derivatives with IC$_{50}$ values < 0.010 μM, in the recombinant human mPGES-1 and in A549 cellular assays. Some of them exhibited striking activity in HWB assay (IC$_{50}$ values < 0.400 μM). The most potent compounds of this series (**120**), (**122**), and (**123**) showed remarkable cell-free mPGES-1 inhibition with IC$_{50}$ of 0.007 μM, 0.005 μM, and 0.010 μM respectively and a potent activity in A549 cell-based assay with IC$_{50}$ of 0.010 μM, 0.005 μM, and 0.011 μM respectively. In HWB assay, they showed IC$_{50}$ of 0.234 μM, 0.376 μM, and 0.328 μM respectively[91]. The mPGES-1 activity of other active compounds is represented in Table **12**.

4.1.14 Carbazole benzamide derivatives

Molecule AF3442 (**122**) **(**Figure **8**) was identified as a potent inhibitor of this series against recombinant mPGES-1 causing selective inhibition of PGE$_2$ biosynthesis by 61±3.3% (mean ± SEM) at 1μM and an IC$_{50}$ value of 0.06 μM. In addition, it inhibited PGE$_2$ production dose-dependently (EC$_{50}$ = 0.41 μM) in LPS-stimulated human monocytes whereas the concentration of other prostanoids (TXB$_2$, PGF2α, and 6-keto-PGF1α) remained unaffected. It exhibited an IC$_{50}$ value of 29 μM in HWB assay[92].

4.1.15 1,2,3-Triazole derivatives

Extensive research has been carried out on the multiple pharmacological actions of 1,2,3-triazole derivatives. Triazoles are known to possess anti-inflammatory[93], anti-tubercular[94,95], anti-cancer[96,97], anti-leishmanial[98], anti-microbial[99], anti-viral[100], and anti-fungal activity[101]. Recent molecular docking studies have shown triazole derivatives as potent mPGES-1 and 5-LOX inhibitors[102]. Based on molecular docking studies compound (**123**) was identified as the lead molecule, showing selective inhibition of PGE$_2$ biosynthesis by 12±3.7% (mean ± SEM) at 30μM and having an IC$_{50}$ of 3.2 μM in a cell-free mPGES-1 inhibitory assay. Substitution of a bulky, halogenated, phenyl ether group on (**123**) increased the

potency and yielded compound (**124**) with an IC_{50} of 0.68 μM[103]. The mPGES-1 inhibitory activity of some compounds of this series is presented in Table **13** and the effect of various substituents on different positions of a 1,2,3-triazole ring on the activity is presented in Figure **9.**

Sulphonamido-1,2,3-triazole derivatives were also reported to be mPGES-1 inhibitors that were designed through fragment-based virtual screening (Figure **10**). The most potent compounds from this series were (**129**) and (**130**) having an IC_{50} of 1.1 μM and 3.3 μM respectively, in a cell-free mPGES-1 inhibitory assay[104].

4.1.16 Endogenous fats, lipids and PGH_2 analogs

Cysteinyl leukotriene C_4 (LTC_4) (**131**) has been reported as a weak inhibitor of mPGES-1 (IC_{50} = 5 μM (Figure **11**). 15-deoxy-$\Delta^{12,14}$-PGJ_2 (**132**) was found to be the most potent inhibitor of mPGES-1 (IC_{50} = 0.3 μM) compared with PGE_2, $PGF_{2\alpha}$, TXB_2, and PGJ_2. A number of fatty acids such as AA (**133**), docosahexaenoic acid (DHA, **134**), eicosapentaenoic acid (EPA, **135**) (IC_{50}= 0.3 μM for each), and palmitic acid (**136**) (IC_{50} = 2 μM) have been reported to possess mPGES-1 inhibitory activity[105].

4.1.17 Anti-inflammatory drugs

Among the known anti-inflammatory drugs and NSAIDs, only sulindac was found to possess a weak mPGES-1 inhibitory action (Figure **12**). Its active metabolite sulindac sulfide (**137**) weakly inhibited mPGES-1 (IC_{50} = 80 μM). A reported COX-2 inhibitor NS-398 (**138**) also inhibited mPGES-1 with an IC_{50} value of 20 μM[106.] Likewise some coxibs such as celecoxib (**139**) (IC_{50} = 22 μM), lumiracoxib (**140**) (IC_{50} = 33 μM), and valdecoxib (**141**) (IC_{50} = 75 μM) also moderately inhibited mPGES-1 activity. A derivative of celecoxib, dimethyl celecoxib (DMC **142**) was also found to be a weak inhibitor of mPGES-1 (IC_{50} = 16 μM)[107].

4.1.18 Miscellaneous inhibitors

There are a number of other synthetic molecules that were discovered through a structure-based virtual screening or were identified as hits in HTS. Compound (**145**), an imidazole amide derivative, showed potent mPGES-1 inhibitory activity (cell-free mPGES-1 IC_{50} = 0.00094 μM, IC_{50} in A549 cells = 0.012 μM, HWB IC_{50} = 0.012 μM)[110]. Further, compound (**148**), a benzimidazole amide derivative showed a distinguished mPGES-1 inhibitory activity (cell-free mPGES-1 IC_{50} = 0.0001 μM, IC_{50} in A549 cells = 0.0012 μM)[113]. Similarly, compound (**164**) also showed mPGES-1 inhibitory activity in nano molar range (cell-free mPGES-1 IC_{50} = 0.0011 μM, HWB IC_{50} = 4.4 μM)[118]. The structure and mPGES-1 inhibitory activity data of other miscellaneous compounds are presented in Table **14**.

4.2 Natural product inhibitors

A few natural product compounds with mPGES-1 inhibitory activity have been reported (Figure **13**). These include curcumin (**175**) (IC_{50} = 0.3 μM) from turmeric[120], epi-gallocatechin gallate (**176**) (IC_{50} = 1.8 μM) from green tea[121], arzanol (**177**) (IC_{50} = 0.4 μM) from *Helichrysum italicum*[122],

garcinol (**178**) (IC_{50} = 0.3 μM) from the fruits of *Guttiferae* species[123], myrtucommulone (**179**) (IC_{50} = 1 μM) from myrtle[124], and hyperforin (**180**) (IC_{50} = 1 μM) from St. John's wort[125]. In addition to these, boswellic acids mainly β-boswellic acid (**181**) (IC_{50} = 5 μM), 11-keto-β-boswellic acid (**182**) (IC_{50} = 10 μM), and 3-O-acetyl-11-keto-β-boswellic acid (**183**) (IC_{50} = 3 μM) from *Boswellia* species (frankincense), moderately inhibited mPGES-1[126]. Also some depsides and depsidones isolated from lichens, physodic acid (**184**) (IC_{50} = 0.43 μM), perlatolic acid (**185**) (IC_{50} = 0.40 μM), and olivetoric acid (**186**) (IC_{50} = 1.15 μM) were also reported to be mPGES-1 inhibitors[127]. Bioactivity-guided fractionation of *Salvia officinalis* revealed the diterpenes carnosol (**187**) and carnosic acid (**188**) as potential bioactive compounds inhibiting mPGES-1 activity with the same IC_{50} value of 5.0 μM[128]. Western blot analysis showed that resveratrol (**189**) dose-dependently reduced the expression (mRNA and protein) of mPGES-1, without affecting the expression of COX-2[129]. Also, some flavonoids like kaempferol (**190**) and isorhamnetin (**191**) were found to downregulate the expression of mPGES-1 in activated macrophages[130].

Conclusions

Recent reports indicate that more than 1.5 billion people worldwide suffer from chronic pain in some form with a direct correlation between incidence rates and increasing age. It is estimated that, at some point in their lives, 20% of the global adult population suffers from pain with 10% of newly diagnosed cases of chronic pain being added each year. The cardiovascular side effects of coxibs and gastro-intestinal side effects of NSAIDs prompted interest in the mPGES-1 as an alternative drug target. Since its discovery, the number of research papers, patents, and reviews has drastically increased in the last 10 years. But till date, there are only a few molecules that could make it to the clinical trials. Molecule LY3023703 by Eli Lilly and Co. entered in phase II clinical trial in August 2013. Another molecule GRC 27864 by Glenmark Pharmaceuticals S.A. entered phase I clinical trials in January 2015 which was estimated to be completed in July 2015. The present review covered 191 synthetic and natural mPGES-1 inhibitors along with their activity profile. Of these, compound (148), a benzimidazole amide derivative was found to be the most potent mPGES-1 inhibitor (cell-free mPGES-1 IC_{50} = 0.0001 μM, IC_{50} in A549 cells = 0.0012 μM). Another compound (145), an imidazole amide derivative, showed potent mPGES-1 inhibitory activity (cell-free mPGES-1 IC_{50} = 0.00094 μM, IC_{50} in A549 cells = 0.012 μM, HWB IC_{50} = 0.012 μM). The present research shows mPGES-1 as a novel and effective drug target for pain and inflammatory therapy that could definitely surpass the side effects of conventional NSAIDs and coxibs. Continuous efforts are being made by many research groups in the direction of improving pharmacokinetic profile of the existing mPGES-1 inhibitors. Looking at the present scenario of continued research efforts on the development of mPGES-1 inhibitors, we can expect a

significant change in the approach of pain and inflammation therapy in the coming years.

References

1. G. Majno and I. Joris, 2nd ed., Oxford University Press: New York, 2004, 307-370.
2. R. Gautam and S.M. Jachak,. *Med. Res. Rev.,* 2009, **29**, 767-820.
3. W.L. Smith, *Biochem. J.,* 1989, **259**, 315–324.
4. S.B. Miller, *Semin. Arthritis Rheum.,* 2006, **36**, 37–49.
5. J.Y. Park, M.H. Pillinger and S.B. Abramson, *Clin. Immunol.,* 2006, **119**, 229–240.
6. C. Funk, Science, 2001, **294**, 1871-75.
7. F. Kojima, S. Kato and S. Kawai, *Fundam. Clin. Pharmacol.,* 2005, **19**, 255-61.
8. H. Futani, A. Okayama, K. Matsui, S. Kashiwamura, T. Sasaki, T. Hada, K. Nakanishi, H. Tateishi, S. Maruo and H. Okamura, *J. Immunother.,* 2002, **25**, 61-64.
9. S. Pugh and G.A. Thomas, *Gut.* 1994, **35**, 675-678.
10. I. Melnikova, *Nat. Rev. Drug Disc.* 2005, **4**, 453-454.
11. L. Marnett, *Annu. Rev. Pharmacol. Toxicol.* 2009, **49**, 265-290.
12. M. Murakami, H. Naraba, T. Tanioka, N. Semmyo, Y. Nakatani, F. Kojima, T. Ikeda, M. Fueki, A. Ueno, S. Oh and I. Kudo, *J. Biol. Chem.,* 2000, **275**, 32783-32792.
13. T. Tanioka, Y. Nakatani, N. Semmyo, M. Murakami and I. Kudo, *J. Biol. Chem.,* 2000, **275**, 32775-32782.
14. P.J. Jakobsson, R. Morgenstern, J. Mancini, A. Ford-Hutchinson and B. Persson, *Protein Sci.,* 1999, **8**, 689–692.
15. P.J. Jakobsson, S. Thoren, R. Morgenstern and B. Samuelsson, *Proc. Natl. Acad. Sci. USA,* 1999, **96**, 7220–7225.
16. C. Jegerschold, S. Pawelzik, P. Purhonen, P. Bhakat, K.R. Gheorghe, N. Gyobu, K. Mitsuoka, R. Morgenstern, P. Jakobsson and H. Hebert, *Proc. Natl. Acad. Sci. USA,* 2008, **105**, 11110-11115.
17. T. Sjogren, J. Nord, M.P. Johansson, G. Liu and S. Geschwindner, *Proc. Natl. Acad. Sci. USA,* 2013, **110**, 3806-3811.
18. K. Watanabe, K. Kurihara, Y. Tokunaga and O. Hayaishi, *Biochem. Biophys. Res. Commun.,* 1997, **235**, 148–152.
19. L. Xing, R.G. Kurumbail, R.B. Frazier, M.S. Davies, H. Fujiwara, R.A. Weinberg, J.K. Gierse, N. Caspers, J.S. Carter, J.J. McDonald, W.M. Moore and M.L. Vazquez, *J. Comput. Aided. Mol. Des.,* 2009, **23**, 13–24.
20. G. Lauro, M. Strocchia, S. Terracciano, I. Bruno, K. Fischer, C. Pergola, O. Werz, R. Riccio and G. Bifulco, *Eur. J. Med. Chem.,* 2014, **80**, 407-415.
21. D.O. Stichtenoth, S. Thoren, H. Bian, M. Peters, P.J. Jakobsson and L.J. Crofford, *J. Immunol.,* 2001, **167**, 469–474.
22. N. Sang, J. Zhang, V. Marcheselli, N.G. Bazan and C. Chen, *J. Neurosci.,* 2005, **25**, 9858–9870.
23. Z. Jia, T. Aoyagi and T. Yang, *Hypertension,* 2010, **55**, 539–546.
24. D.M. Duffy, C.L. Seachord and B.L. Dozier, *Hum. Reprod.,* 2005, **20**, 1485–1492.
25. S. Bombardieri, P. Cattani, G. Ciabattoni, O. Munno, G. Pasero, C. Patrono, E. Pinca and F. Pugliese, *Br. J. Pharmacol.,* 1981, **73**, 893–901.
26. K. Subbaramaiah, K. Yoshimatsu, E. Scherl, K.M. Das, K.D. Glazier, D. Golijanin, R.A. Soslow, T. Tanabe, H. Naraba and A.J. Dannenberg, *J. Biol. Chem.,* 2004, **279**, 12647-12658.
27. M.M. Hardy, K. Seibert, P.T. Manning, M.G. Currie, B.M. Woerner, D. Edwards, A. Koki and C.S. Tripp, *Arthritis Rheum.,* 2002, **46**, 1789–1803.
28. R.W. Friesen and J.A. Mancini, *J. Med. Chem.,* 2008, **51**, 4059-4067.
29. H.F. Liu, X.H. Li, Q.D. Yang, W. Miao, S.S. Qi, X.M. Song, G.S. He, H.L. Dong and F.Q. Zhang, *Chinese. J. Med. Genet.,* 2007, **24**, 453–456.
30. K. Nonaka, H. Fujioka, Y. Takii, S. Abiru, K. Migita, M. Ito T. Kanematsu, and H. Ishibashi, *World J. Gastroenterol.,* 2010, **16**, 4846–4853.
31. H.H. Chang and E.J. Meuillet, *Future Med. Chem.,* 2011, **3**, 1909-1934.
32. B.H. Von, H.J. Stein, S.A. Hartl, J. Theisen, B. Stigler, J.R. Siewert and M. Sarbia, *Dis. Esophagus.,* 2008, **21**, 304–308.
33. G. Nardone, A. Rocco, D. Vaira, S. Staibano, A. Budillon, F. Tatangelo, M.G. Sciulli, F. Perna, G. Salvatore, M. Di Benedetto, G. De Rosa and P. Patrignani, *J. Pathol.,* 2004, **202**, 305–312.
34. T.J. Jang, *Virchows. Arch.,* 2004, **445**, 564–571.
35. K. Gudis, A. Tatsuguchi, K. Wada, T. Hiratsuka, S. Futagami, Y. Fukuda, T. Kiyama, T. Tajiri, K. Miyake and C. Sakamoto, *Hum. Pathol.,* 2007, **38**, 1826–1835.
36. A. Rocco, R. Caruso, L. Toracchio, L. Rigoli, F. Verginelli, T. Catalano, M. Neri, M.C. Curia, L. Ottini, V. Agnese, V. Bazan, A. Russo, G. Pantuso, G. Colucci, R. Mariani-Costantini and G. Nardone, *Ann. Oncol.,* 2006, **17**, 103–108.
37. K. Yoshimatsu, D. Golijanin, P.B. Paty, R.A. Soslow, P.J. Jakobsson, R.A. DeLellis, K. Subbaramaiah and A.J. Dannenberg, *Clin. Cancer Res.,* 2001, **7**, 3971–3976.
38. S.C. Lim, H. Cho, T.B. Lee, C.H. Choi, Y.D. Min, S.S. Kim and K.J. Kim, *Yonsei. Med. J.,* 2010, **51**, 692–699.
39. Y. Takii, S. Abiru, H. Fujioka, M. Nakamura, A. Komori, M. Ito, K. Taniguchi, M. Daikoku, Y. Meda, K. Ohata, K. Yano, S. Shimoda, H. Yatsuhashi, H. Ishibashi and K. Migita, *Liver. Int.,* 2007, **27**, 989–996.
40. K. Nonaka, H. Fujioka, Y. Takii, S. Abiru, K. Migita, M. Ito, T. Kanematsu and H. Ishibashi, *World J. Gastroenterol.,* 2010, **16**, 4846–4853.
41. S. Hasan, M. Satake, D. Dawson, H. Funahashi, E. Angst, V.L. Go, H.A. Reber, O.J. Hines and G. Eibl, *Pancreas.,* 2008, **37**, 121–127.
42. S. Mattila, H. Tuominen, J. Koivukangas and F. Stenback, *Neuropathology,* 2009, **29**, 156–165.
43. N. Baryawno, B. Sveinbjornsson, S. Eksborg, A. Orrego, L. Segerstrom, C.O. Oqvist, S. Holm, B. Gustavsson, B. Kagedal, P. Kogner and J.I. Johnsen, *Neuro. Oncol.,* 2008, **10**, 661–674.
44. S. Mehrotra, A. Morimiya, B. Agarwal, R. Konger and S. Badve, *J. Pathol.,* 2006, **208**, 356–363.
45. Z. Gatalica, S.L. Lilleberg, M.S. Koul, T. Vanecek, O. Hes, B. Wang and M. Michal, *Hum. Pathol.,* 2008, **39**, 1495–1504.
46. Y. Omi, N. Shibata, T. Okamoto, T. Obara and M. Kobayashi, *Acta. Histochem. Cytochem.,* 2009, **42**, 105–109.
47. R. Kawata, S. Hyo, M. Araki and H. Takenaka, *Auris. Nasus. Larynx.,* 2010, **37**, 482–487.
48. E.G. Cohen, T. Almahmeed, B. Du, D. Golijanin, J.O. Boyle, R.A. Soslow, K. Subbaramaiah and A.J. Dannenberg, *Clin. Cancer Res.,* 2003, **9**, 3425–3430.
49. D. Golijanin, J.Y. Tan, A. Kazior, E.G. Cohen, P. Russo, G. Dalbagni, K.J. Auborn, K. Subbaramaiah and A.J. Dannenberg, *Clin. Cancer Res.* 2004, **10**, 1024–1031.

ARTICLE

50. K. Yoshimatsu, N.K. Altorki, D. Golijanin, F. Zhang, P.J. Jakobsson, A.J. Dannenberg and K. Subbaramaiah, *Clin. Cancer Res*., 2001, **7**, 2669–2674.
51. Y.C. Wu, L.J. Su, H.W. Wang, C.F. Jeff Lin, W.H. Hsu, T.Y. Chou, C.Y. Huang, C.L. Lu and C.T. Hsueh, *J. Thorac. Oncol*., 2010, **5**, 1167–1174.
52. H.W. Wang, C.T. Hsueh, C.F. Lin, T.Y. Chou, W.H. Hsu, L.S. Wang and Y.C. Wu, *Ann. Surg. Oncol*., 2006, **13**, 1224–1234.
53. R. Kawata, S. Hyo, T. Maeda, Y. Urade and H. Takenaka, *Acta. Otolaryngol.,* 2006, **126***,* 627–632.
54. M. Herfs, L. Herman, P. Hubert, F. Minner, M. Arafa, P. Roncarati, Y. Henrotin, J. Boniver and P. Delvenne, *Cancer Immunol. Immunother*., 2009, **58**, 603–614.
55. H.N. Jabbour, S.A. Milne, A.R. Williams, R.A. Anderson and S.C. Boddy, *Br. J. Cancer.*, 2001, **85**, 1023–1031.
56. K. Rask, Y. Zhu, W. Wang, L. Hedin and K. Sundfeldt, *Mol. Cancer*., 2006, **5**, 62-67.
57. P.J. Cimino, C.D. Keene, R.M. Breyer, K.S. Montine and T.J. Montine, *Curr. Med. Chem.,* 2008, **15**, 1863–1869.
58. M. Wang, A.M. Zukas, Y. Hui, E. Ricciotti, E. Pure and G.A. Fitzgerald, *Proc. Natl. Acad. Sci. USA,* 2006, **103***,* 14507–14512.
59. E.J. Corey, K.C. Nicolaou, Y. Machida, C.L. Malmsten and B. Samuelsson, *Proc. Natl. Acad. Sci. U.S.A.,* 1975, **72**, 3355–3358.
60. A. Koeberle, U. Siemoneit, U. Buhring, H. Northoff, S. Laufer, W. Albrecht and O. Werz, *J. Pharmacol. Exp. Ther*., 2008, **326**, 975–982.
61. T. Hammarberg, M. Hamberg, A. Watterholm, H. Hansson, B. Samuelsson and Z. Haeggstrom, *J. Biol. Chem*., 2009, **284**, 301–305.
62. M. Ouellet, J.P. Falgueyret, P.H. Ear, A. Pen, J.A. Mancini, D. Riendeau, and M.D. Percival, *Protein Expr. Purif*., 2002, **26**, 489–495.
63. S. Thoren, R. Weinander, S. Saha, C. Jegerschold, P.L. Pettersson, B. Samuelsson, H. Hebert, M. Hamberg, R. Morgenstern and P. Jakobsson, *J. Biol. Chem.,* 2003, **278**, 22199-22209.
64. T. Sjogrena, J. Nord, M. Eka, P. Johanssona, G. Liub and S. Geschwindner, *Proc. Natl. Acad. Sci. U S A*., 2013, **110**, 3806–3811.
65. W. Kim, K. Choi, H.S. Do and Y.G. Yu, *BMB Rep*., 2008, **41**, 808-13.
66. D. Schwarz, F. Junge, F. Durst, N. Frolich, B. Schneider, S. Reckel, S. Sobhanifar, V. Dotsch and F. Bernhard, *Nat. Protoc.,* 2007*,* **2,** 2945–2957.
67. L. Harding, Z. Wang and H. Tai, *Biochimica. Et. Biophysica. Acta*., 1996, **1310**, 48-52.
68. E.R. Goedken, A.I. Gagnon, G.T. Overmeyer, J. Liu, R.A. Petrillo, A.F. Burchat and M.J. Tomlinson, *J. Biomol. Screen*., 2008, **13**, 619-625.
69. A. Koeberle, A. Rossi, H. Zettl, C. Pergola, F. Dehm, J. Bauer, C. Greiner, S. Reckel, C. Hoernig, H. Northoff, F. Bernhard, L. Sautebin, M.S. Zsilavecz and O. Werz, *J. Pharmacol. Exp. Ther.,* 2010*,* **332***,* 840–848.
70. A. Koeberle, E.M. Haberl, A. Rossi, C. Pergola, F. Dehma, H. Northoff, R. Troschuetz, L. Sautebin and O. Werz, *Bioorg. Med. Chem.,* 2009, **17**, 7924–7932.
71. J. Wang, D. Limburg, J. Carter, G. Mbalaviele, J. Gierse and M. Vazquez, *Bioorg. Med. Chem. Lett*., 2010, **20**, 1604-1609.
72. G. Mbalaviele, A.M. Pauley, A.F. Shaffer, B.S. Zweifel, S. Mathialagan, S.J. Mnich, O.V. Nemirovskiy, J. Carter, J.L. Gierse, M.L. Vazquez and W.M. Moore, *Biochem. Pharmacol*., 2010, **79**, 1445-54.
73. M.D. Guerrero, M. Aquino, I. Bruno, M.C. Terencio, M. Paya, R. Riccio and L. Gomez-Paloma, *J. Med. Chem*., 2007, **50**, 2176–2184.
74. A.J. Liedtke, P. Keck, F. Lehmann, A. Koeberle, O. Werz and S.A. Laufer, *J. Med. Chem*., 2009, **52**, 4968–4972.
75. T.Y. Wu, H. Juteau, Y. Ducharme, R.W. Friesen, S. Guiral, L. Dufresne, H. Poirier, M. Salem, D. Riendeau and J. Mancini, *Bioorg. Med. Chem. Lett*., 2010, **20**, 6978-6982.
76. J. G. Luz, S. Antonysamy, B. Condon, M. Lee, A. Zhang, M. Russell, S.S. Chang, D. Allison, M.J. Fisher, S.L. Kuklish, X. Yu, A. Sloan, R. Backer, A. Harvey, and S. Chandrasekhar, *J. Med. Chem*., 2015, **58**, 4727–4737.
77. J.A. Mancini, K. Blood, J. Guay, R. Gordon, D. Claveau, C.C. Chan and D. Riendeau, *J. Biol. Chem*., 2001, **276**, 4469-75.
78. D. Riendeau, R. Aspiotis, D. Ethier, Y. Gareau, G.L. Grimm, J. Guay, J. Rubin and R.E. Friesen, *Bioorg. Med. Chem. Lett*., 2005, **15**, 3352–3355.
79. J. Landwehr, S. George, E.M. Karg, D. Poeckel, D. Steinhilber, R. Troschuetz and O. Werz, *J. Med. Chem*., 2006, **49**, 4327-32.
80. G.B. Arhancet, D.P. Walker, S. Metz, Y.M. Fobian, S.E. Heasley, D. Jones, M.J. Hayes, J.S. Carter, J.R. Springer, H.F. Lu, A.F. Shaffer, G.M. Jerome, M.T. Baratta, B.S. Zweifel, W.M. Moore, J.L. Masferrer and M.L. Vazquez, *Bioorg. Med. Chem. Lett*., 2013, **23**, 1120-26.
81. B. Cote, L. Boulet, C. Brideau, D. Claveau, D. Ethier, R. Frenette, M. Gagnon, A. Giroux, J. Guay, S. Guiral, J. Mancini, E. Martins, F. Masse, N. Méthot, D. Riendeau, J. Rubin, D. Xu, H. Yu, Y. Ducharme and R.W. Friesen, *Bioorg. Med. Chem. Lett.,* 2007, **17**, 6816-20.
82. A. Giroux , L. Boulet, C. Brideau, A. Chau, D. Claveau, B. Cote, D. Ethier, R. Frenette, M. Gagnon, J. Guay, S. Guiral, J. Mancini, E. Martins, F. Masse, N. Methot, D. Riendeau, J. Rubin, D. Xu, H. Yu, Y. Ducharme and R.W. Friesen, *Bioorg. Med. Chem. Lett.,* 2009, **19**, 5837–5841.
83. T. Shiro, K. Kakiguchi, H. Takahashi, H. Nagata and M. Tobe, *Bioorg. Med. Chem. Lett*., 2012, **22**, 285–288.
84. T. Shiro, K. Kakiguchi, H. Takahashi, H. Nagata and M. Tobe, *Bioorg. Med. Chem*., 2013, **21**, 2068–2078.
85. T. Shiro, K. Kakiguchi, H. Takahashi, H. Nagata and M. Tobe, *Bioorg. Med. Chem*., 2013, **21**, 2868-2878.
86. A. Wiegard, W. Hanekamp, K. Griessbach, J. Fabian and M. Lehr, *Eur. J. Med. Chem.,* 2012, **48**, 153-163.
87. J.F. Chiasson, L. Boulet, C. Brideau, A. Chau, D. Claveau, B. Cote, D. Ethier, A. Giroux, J. Guay, S. Guiral, J. Mancini, F. Masse, N. Methot, D. Riendeau, P. Roy, J. Rubin, D. Xu, H. Yu, Y. Ducharme and R.W. Friesen, *Bioorg. Med. Chem. Lett.,* 2011, **21**, 1488-1492.
88. A. Koeberle, H. Zettl, C. Greiner, M. Wurglics, M.S. Zsilavecz and O. Werz, *J. Med. Chem.,* 2008**, 51***,* 8068–8076.
89. T. Hanke, F. Dehm, S. Liening, S.D. Popella, J. Maczewsky, M. Pillong, J. Kunze, C. Weinigel, D. Barz, A. Kaiser, M. Wurglics, M. Lammerhofer, G. Schneider, L. Sautebin, M.S. Zsilavecz and O. Werz, *J. Med. Chem*., 2013, **56**, 9031–9044.
90. C. Greiner, H. Zettl, A. Koeberle, C. Pergola, H. Northoff, M. Schubert-Zsilavecz and O. Werz, *Bioorg. Med. Chem*., 2011, **19**, 3394–3401.
91. A. Banerjee, M.Y. Pawar, S. Patil, P.S. Yadav, P.A. Kadam, V.G. Kattige, D.S. Deshpande, P.V. Pednekar, M.K. Pisat and L.A. Gharat, *Bioorg. Med. Chem. Lett.,* 2014**, 24,** 4838–4844.
92. A. Bruno, L. Francesco, I. Coletta, G. Mangano, M.A. Alisi, L. Polenzani, C. Milanese, P. Anzellotti, E. Ricciotti,

M. Dovizio, A. Di Francesco, S. Tacconelli, M.L. Capone and P. Patrignani, *Biochem. Pharmacol.*, 2010, **79**, 974–981.

93. S. Haider, M.S. Alam, H. Hamid, S. Shafi, A. Nargotra, P. Mahajan, S. Nazreen, A.M. Kalle, C. Kharbanda, Y. Ali, A. Alam and A.K. Panda, *Eur. J. Med. Chem.*, 2013, **70**, 579-588.

94. J.P. Sridevi, P. Yogeeswari, D. Sriram and S. Kantevari, *Eur. J. Med. Chem.,* 2014, **71**, 160-167.

95. C. Menendez, A. Chollet, F. Rodriguez, C. Inard, M.R. Pasca and C. Lherbet, *Eur. J. Med. Chem.,* 2012, **52**, 275-283.

96. H. Elamari, R. Slimi, G.G. Chabot, L. Quentin, D. Scherman and C. Girard, *Eur. J. Med. Chem.,* 2013, **60**, 360-364.

97. A. Kamal, S. Prabhakar, M.J. Ramaiah, P.V. Reddy, C.R. Reddy, A. Mallareddy, N. Shankaraiah, T. Lakshmi Narayan Reddy, S.N. Pushpavalli and M. Pal-Bhadra, *Eur. J. Med. Chem.,* 2011, **46**, 3820-3831.

98. T.T. Guimaraes, F.R. Pinto, J.S. Lanza, M.N. Melo, R.L. Neto, I.M. Melo, E.B. Diogo, V.F. Ferreira, C.A. Camara, W.O. Valença, R.N. de Oliveira, F. Frézard and E.N. da Silva Jr*, Eur. J. Med. Chem.,* 2013, **63**, 523-530.

99. B. Garudachari, A.M. Isloor, M.N. Satyanarayana, H.K. Fun and G. Hegde, *Eur. J. Med. Chem.,* 2014, **74**, 324-332.

100. F. Silva, M.C. Souza, I.I.P. Frugulhetti, H.C. Castro, S.L. Souza, T.M. Souza, D.Q. Rodrigues, A.M. Souza, P.A. Abreu, F. Passamani, C.R. Rodrigues and V.F. Ferreira, *Eur. J. Med. Chem.,* 2009, **44**, 373-383.

101. X.L. Wang, K. Wan and C.H. Zhou, *Eur. J. Med. Chem.,* 2010, **45**, 4631-4639.

102. R.D. Simone, M.G. Chini, I. Bruno, R. Riccio, D. Mueller, O. Werz and G. Bifulco, *J. Med. Chem.*, 2011, **54**, 1565–1575.

103. M.G. Chini, R.D. Simone, R. Riccio, F. Dehmb, O. Werz and C. Bifulco. *Eur. J. Med. Chem.*, 2012, **54**, 311-323.

104. K. Lee, V.C. Pham, M.J. Choi, K.J. Kim, K. Lee, S. Han, Y.G. Yu and J.Y. Lee, *Bioorg. Med. Chem. Lett.,* 2013*,* **23***,* 75–80.

105. O. Quraishi, J.A. Mancini and D. Riendeau, *Biochem. Pharmacol.*, 2002, **63**, 1183-9.

106. S. Thoren and P.J. Jakobsson, *Eur. J. Biochem.*, 2000, **267**, 6428–6434.

107. I. Wobst, S. Schiffmann, K. Birod, T.J. Maier, R. Schmidt, C. Angioni, G. Geisslinger, and S. Grosch, *Biochem. Pharmacol.*, 2008, **76**, 62–69.

108. J. Bylund, M. Ek, J. Holenz, M.H. Johansson, A. Kers, K. Narhi, G. Nordvall, L. Ohberg. D. Sohn, J. Viklund and S. Berg, *PCT Intl. Appl.*, WO/2009/064250, 2009.

109. R. Pfau, K. Arndt, H. Doods, K. Klinder, R. Kuelzer, D. Lubriks, J. Mack, B. Pelcman, H. Priepke, R. Roenn, D. Stenkamp and E. Suna, PCT Intl. Appl., WO/2010/100249, 2010.

110. N.E. Hughes, T.A. Woods and B.H. Norma, PCT Intl. Appl., WO/2012/161965, 2012.

111. J. Wannberb, M. Alterman, P. Stenberg and J. Westman, PCT Intl. Appl., WO/2009/103778, 2009**.**

112. H. Priepke, H. Doods, R. Kuelzer, R. Pfau, D. Stenkamp, R. Roenn and B. Pelcman, PCT Intl. Appl., WO/2011/048004, 2011.

113. H. Otsu, PCT Intl. Appl., WO/2013/024898, 2013.

114. A. Hamza, X. Zhao, M. Tong, H. Tai and C. Zhan, *Bioorg. Med. Chem.,* 2011, **19***,* 6077–6086.

115. B. Waltenberger, K. Wiechmann, J. Bauer, P. Markt, S.M. Noha, G. Wolber, J.M. Rollinger, O. Werz, D. Schuster and H. Stuppner, *J. Med. Chem.*, 2011, **54**, 3163–3174.

116. S. Park, S. Han, H.M. Ahsan, K. Lee, J.Y. Lee, J. Shin, K. Lee, N. Kang and Y.G. Yu, *Bioorg. Med. Chem. Lett.,* 2012**, 22**, 7335–7339.

117. M. Hieke, C. Greiner, M. Dittrich, F. Reisen, G. Schneider, M.S. Zsilavecz and O. Werz, *J. Med. Chem.*, 2011, **54***,* 4490–4507.

118. S. He, C. Li, Y. Liu and L. Lai, *J. Med. Chem.*, 2013, **56***,* 3296–3309.

119. R.D. Simone, I. Bruno, R. Riccio, K. Stadler, J. Bauer, A.M. Schaible, S. Laufer and O. Werz, *Bioorg. Med. Chem.*, 2012, **20**, 5012–5016.

120. A. Koeberle, H. Northoff and O. Werz, *Mol. Cancer Ther.,* 2009, **8**, 2348–2355.

121. A. Koeberle, J. Bauer, M. Verhoff, M. Hoffmann, H. Northoff and O. Werz, *Biochem. Biophys. Res. Commun.,* 2009, **388**, 350-4.

122. J. Bauer, A. Koeberle, F. Dehm, F. Pollastro, G. Appendino, H. Northoff, A. Rossi, L. Sautebin, and O. Werz, *Biochem. Pharmacol.,* 2011, **81**, 259–268.

123. A. Koeberle, H. Northoff and O. Werz, *Biochem. Pharmacol.*, 2009, **77**, 1513–1521.

124. A. Koeberle, F. Pollastro, H. Northoff and O. Werz, *Br. J. Pharmacol.*, 2009, **156**, 952–961.

125. A. Koeberle, A. Rossi, J. Bauer, F. Dehm, L. Verotta, H. Northoff, L. Sautebin and O. Werz, *Front. Pharmacol.*, 2011, **2**, 7-11.

126. U. Siemoneit, A. Koeberle, A. Rossi, F. Dehm, M. Verhoff, S. Reckel, T.J. Maier, J. Jauch, H. Northoff, F. Bernhard, V. Doetsch, L. Sautebin and O. Werz, *Br. J. Pharmacol.*, 2011, **162**, 147–162.

127. J. Bauer, B. Waltenberger, S.M. Noha, D. Schuster, J.M. Rollinger, J. Boustie, M. Chollet, H. Stuppner and O. Werz, *Chem. Med. Chem.*, 2012, **7**, 2077 – 2081.

128. J. Bauer, S. Kuehnl, J.M. Rollinger, O. Scherer, H. Northoff, H. Stuppner, O. Werz and A. Koeberle, *J. Pharmacol. Exp. Ther.*, 2012, **342**, 169-76.

129. E.C. Jalil, A.C. Pinheiro, S. Graf, H.S. Bhatia, M. Hull, E. Munoz and B.L. Fiebich, *J. Neuroinflamm.,* 2007, **4**, 25-37.

130. M. Hamalainen, R. Nieminen, M.Z. Asmawi, P. Vuorela, H. Vapaatalo and E. Moilanen, *Planta Med.*, 2011, **77**, 1504–1511.
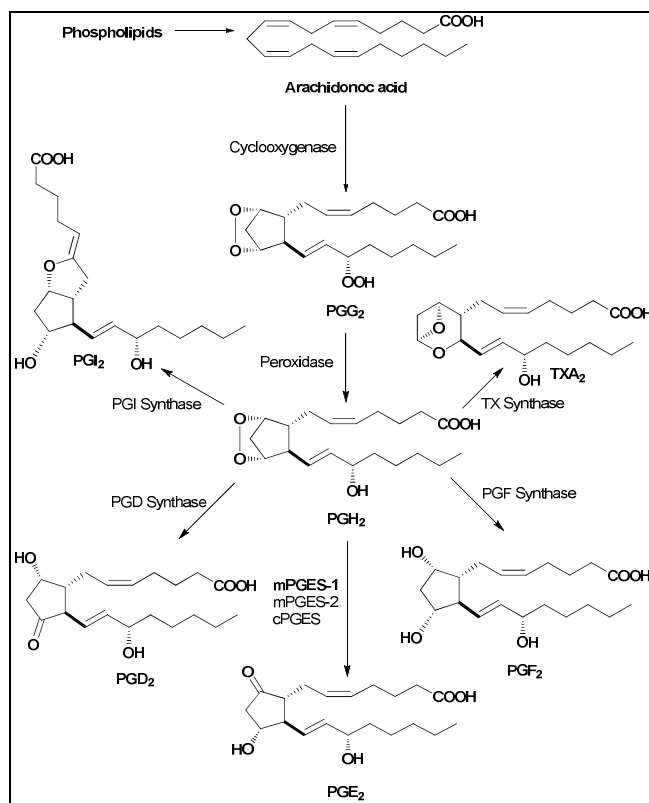
Figure 1: Prostaglandin synthesis pathway
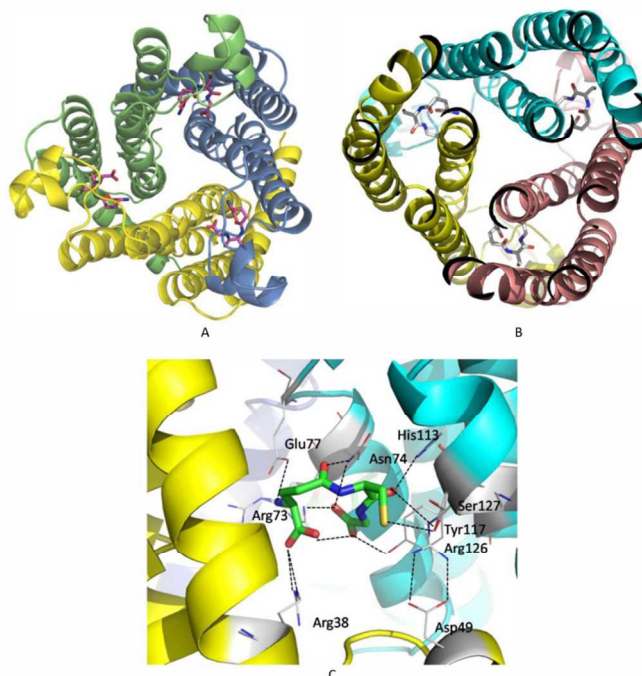
Figure 2: **(A)** Structure of mPGES-1 (side view) (PDB: 4ALO); **(B)** Top view; **(C)** Binding mode of GSH to mPGES-1[17].
Image reprinted with permission from T. Sjogren, J. Nord, M.P. Johansson, G. Liu and S. Geschwindner, *Proc. Natl. Acad. Sci. USA,* 2013, **110**, 3806-3811. Copyright (2016) National Academy of Sciences.
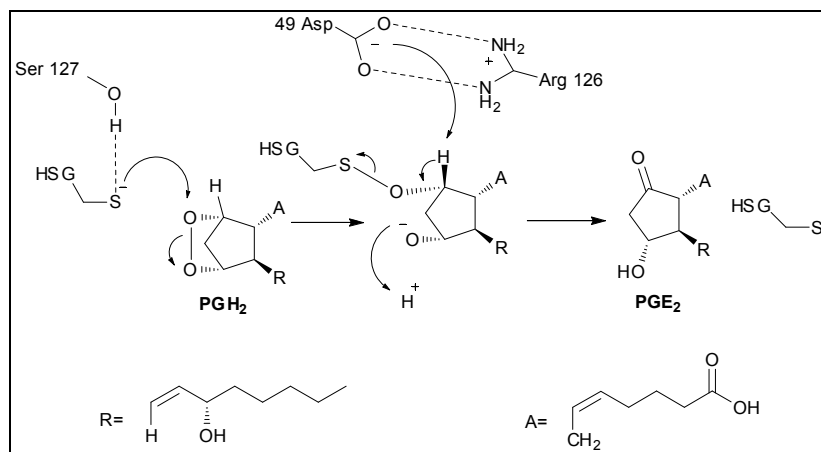
Figure 3: Proposed mechanism of action of mPGES-1
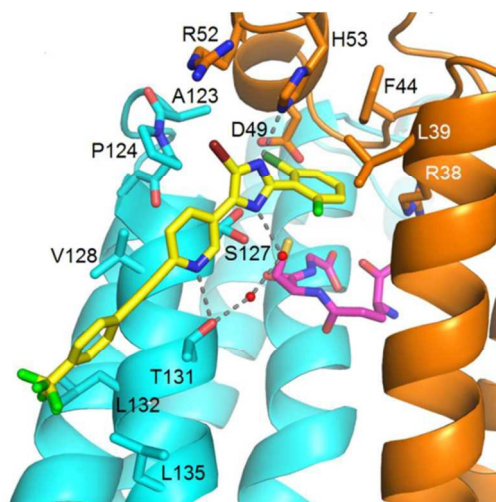
Figure 4: Binding mode of **11** to mPGES-1[76].

Image reprinted with permission from J. G. Luz, S. Antonysamy, B. Condon, M. Lee, A. Zhang, M. Russell, S.S. Chang, D. Allison, M.J. Fisher, S.L. Kuklish, X. Yu, A. Sloan, R. Backer, A. Harvey, and S. Chandrasekhar, *J. Med. Chem.*, 2015, **58**, 4727–4737. Copyright (2016) American Chemical Society.
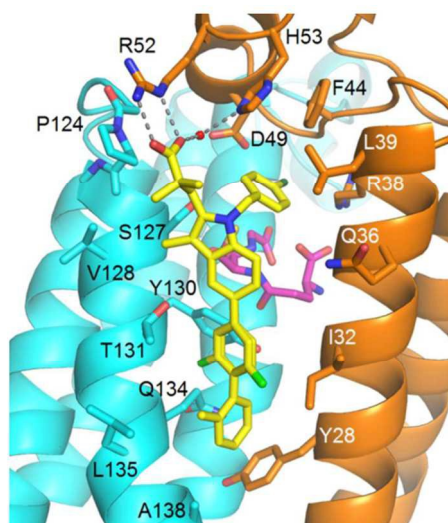
Figure 5: Binding mode of **17** to mPGES-1[76].

Image reprinted with permission from J. G. Luz, S. Antonysamy, B. Condon, M. Lee, A. Zhang, M. Russell, S.S. Chang, D. Allison, M.J. Fisher, S.L. Kuklish, X. Yu, A. Sloan, R. Backer, A. Harvey, and S. Chandrasekhar, *J. Med. Chem.*, 2015, **58**, 4727–4737. Copyright (2016) American Chemical Society.
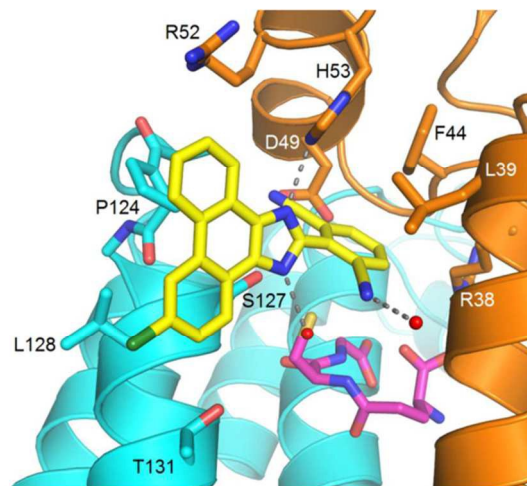
Figure 6: Binding mode of **44** to mPGES-1[76].
Image reprinted with permission from J. G. Luz, S. Antonysamy, B. Condon, M. Lee, A. Zhang, M. Russell, S.S. Chang, D. Allison, M.J. Fisher, S.L. Kuklish, X. Yu, A. Sloan, R. Backer, A. Harvey, and S. Chandrasekhar, *J. Med. Chem*., 2015, **58**, 4727–4737. Copyright (2016) American Chemical Society.
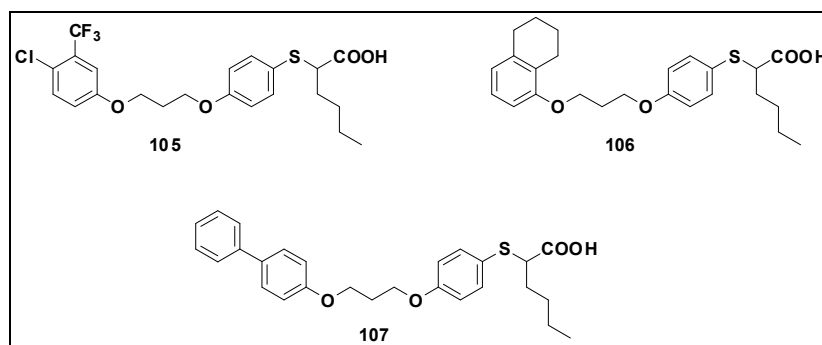
Figure 7: 2-Mercaptohexanoic acid derivatives.
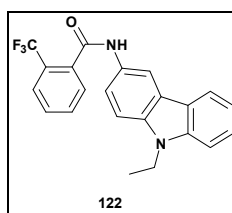
Figure 8: Carbazole benzamide derivative AF3442
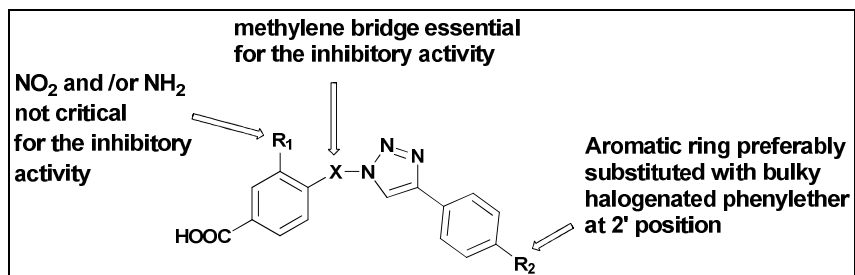
Figure 9: Effect of various substituents on different positions of a 1,2,3-triazole ring on mPGES-1 inhibitory activity.
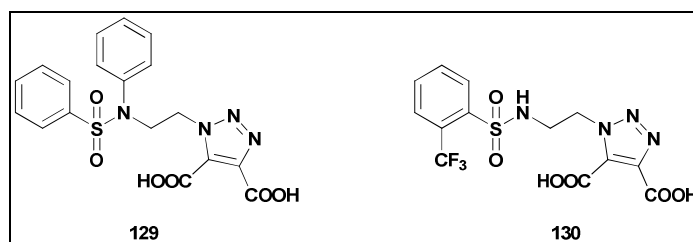
Figure 10: Sulphonamido-1,2,3-triazole derivatives
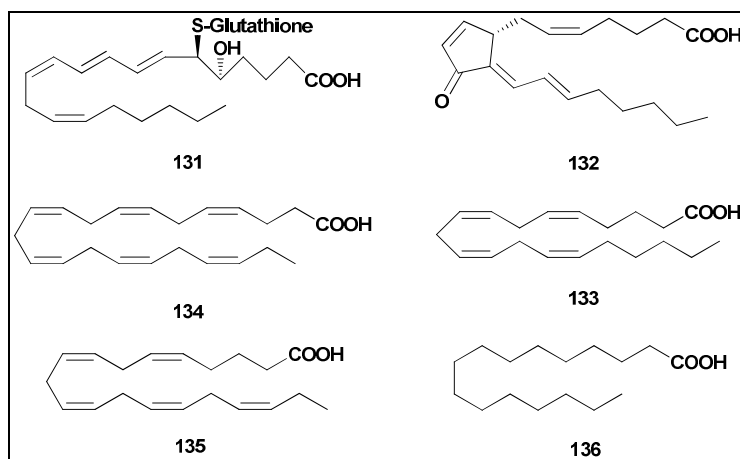
Figure 11: Endogenous fats, lipids and PGH$_2$ analogues having mPGES-1 inhibitory activity
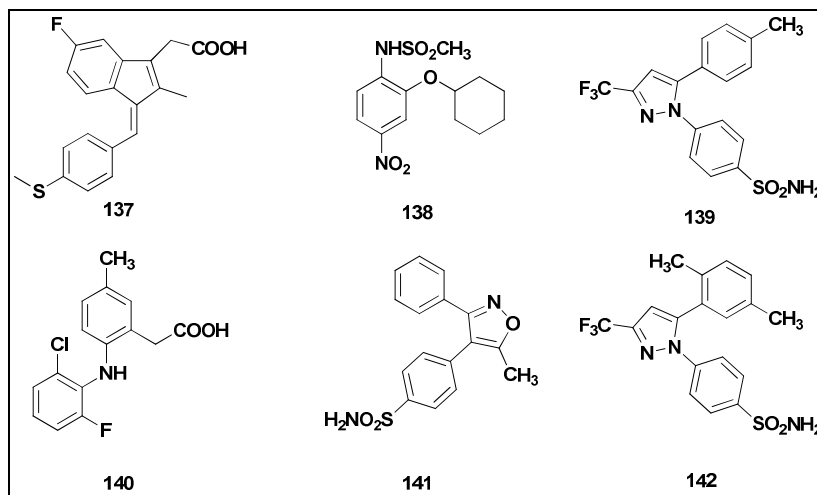
Figure 12: Anti-inflammatory drugs having mPGES-1 inhibitory activity
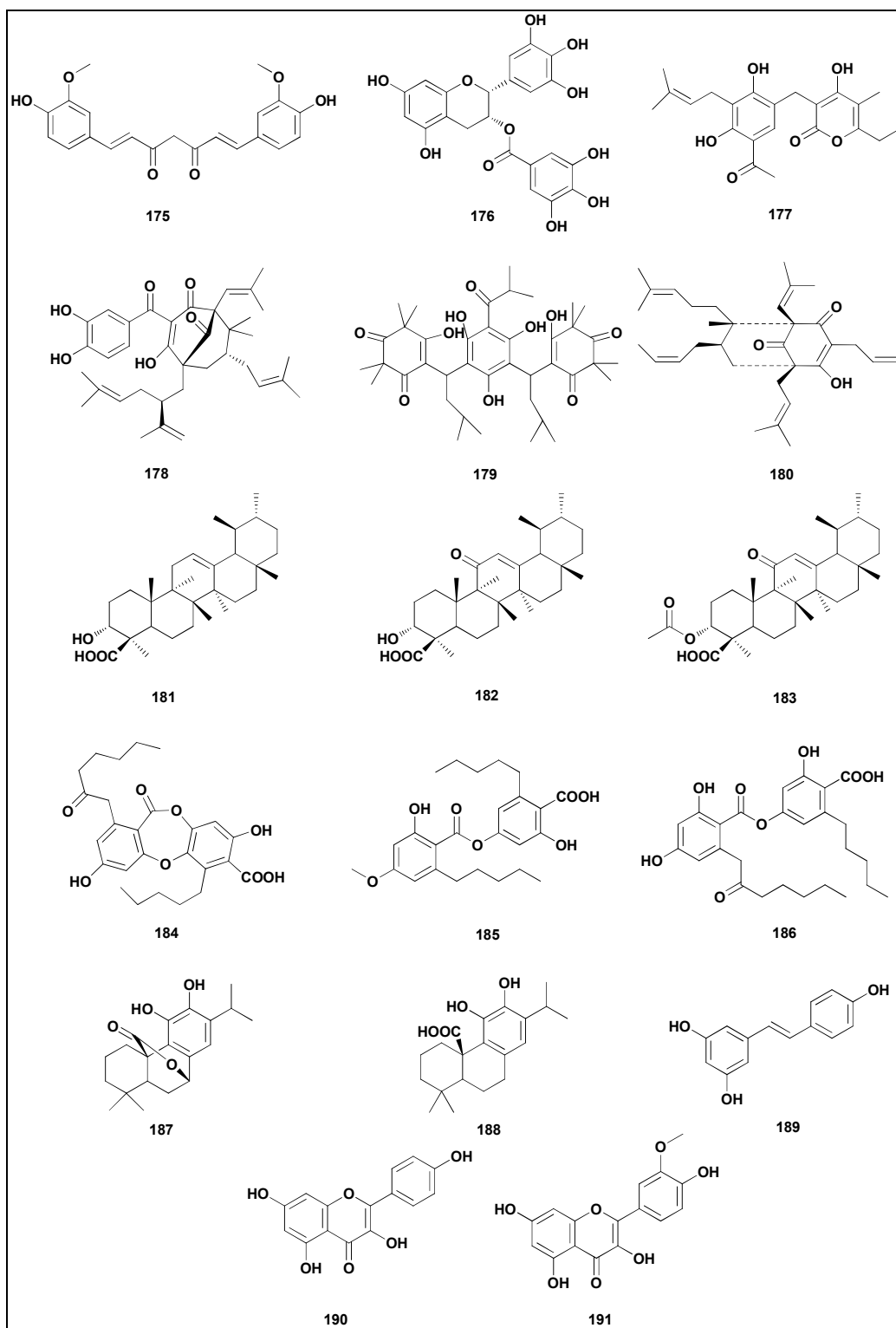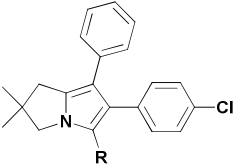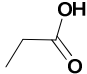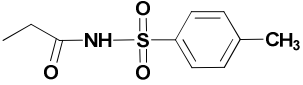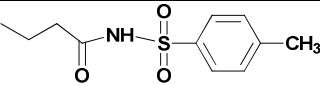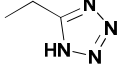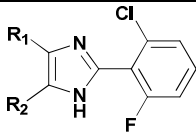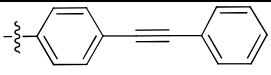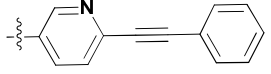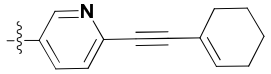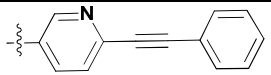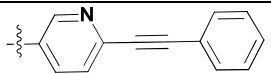
Figure 13: Natural product inhibitors of mPGES-1

Compound	R	mPGES-1 IC$_{50}$ (µM)	Cell free mPGES-1 residual activity at 10 µM (% PGE$_2$ of control) (±SEM)
1		6.7	44.9±2.6
2		4.8	32.2±0.9
3		2.1	23.2±1.9
4		3.9	27.9±7.2

SEM = Standard Error of Mean

Table1: mPGES-1 inhibitory activity of Arylpyrrolizines
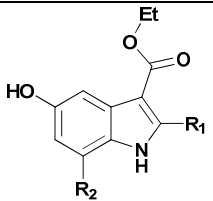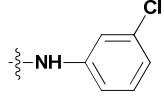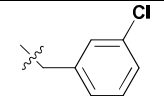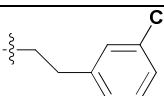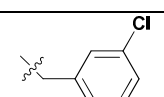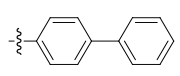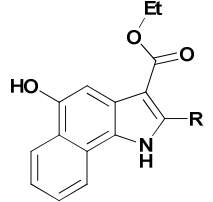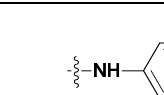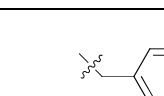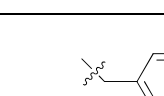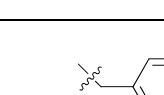
Compound	R$_1$	R$_2$	mPGES-1 IC$_{50}$ (µM)
5		H	0.660
6		H	0.008
7		H	0.023
8		H	0.013
9		Cl	0.005
10		Br	0.001

| 11 | | Br | 0.0073 |

Table 2: mPGES-1 inhibitory activity of biarylimidazoles

Compound	R$_1$	R$_2$	mPGES-1 IC$_{50}$ (µM)
12 (MK886)			1.6
13		-CH$_3$	1
14		-CH$_3$	0.16
15		-CH$_3$	0.016
16		-CH$_3$	0.007
17		-CH$_3$	0.003

Table 3: mPGES-1 inhibitory activity of MK-886 derivatives

Compound	R$_1$	R$_2$	mPGES-1 IC$_{50}$ (µM)	Cell free mPGES-1 residual activity at 10 µM (% PGE$_2$ of control) (±SEM)
18		H	n.d.	83±8
19		H	n.d.	55±10
20		H	n.d.	65±6
21			3.1	25±2

Compound	R	mPGES-1 IC$_{50}$ (µM)	Cell free mPGES-1 residual activity at 10 µM (% PGE$_2$ of control) (±SEM)
22		1.6	13±4
23		0.6	3±2
24		0.5	5±2
25		0.2	14±5

26		0.6	9±1
27		0.1	14±0

n.d.= not determined, SEM = Standard Error of Mean

Table 4: mPGES-1 inhibitory activity of Benzo[g]indol-3-carboxylate derivatives

Compound	R	mPGES-1 IC$_{50}$ (µM)
28		1.2
29		0.85
30		0.82
31		0.24
32		0.29
33		0.82
34		0.17
35		0.38
36		>19.1
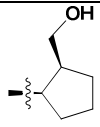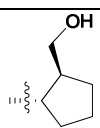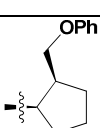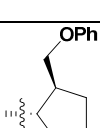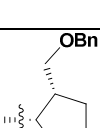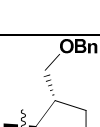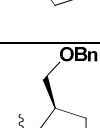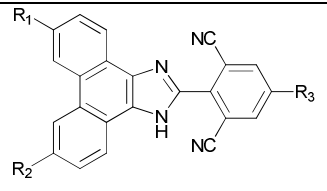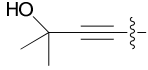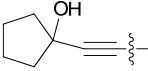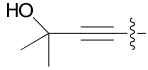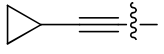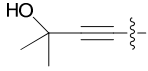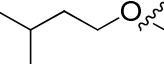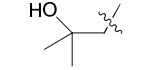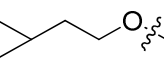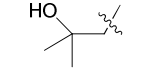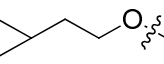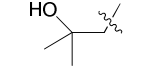
37		0.78
38		3.2
39		0.043
40		0.034
41		0.082
42		0.04
43		0.018
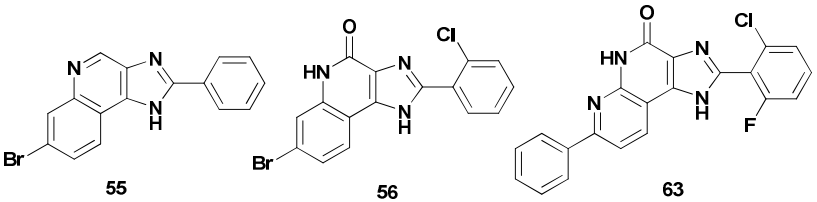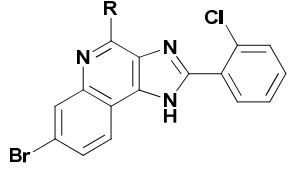
Table 5: mPGES-1 inhibitory activity of Benzoxazole derivatives

Compound	R_1	R_2	R_3	Cell free mPGES-1 inhibition	PGE$_2$ inhibition in A549 cells	PGE$_2$ inhibition in HWB
					IC$_{50}$ (µM)	
44	Cl	H	H	0.001	0.42	1.3

45	Cl	OH(CH$_3$)$_2$C	H	0.004	0.034	1.4
46	Cl	NC(CH$_2$)$_3$O	H	0.001	0.038	0.38
47	Cl	4-Pyridyl C≡C	H	0.001	0.075	0.39
48	Cl		H	0.001	0.013	0.20
49	Cl		H	0.001	0.027	0.26
50	Ethyl		H	0.001	-	0.37
51			H	0.001	-	0.076
52			H	0.0004	-	0.15
53			H	0.0009	-	0.22
54			F	0.001	-	0.14
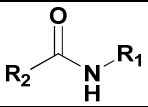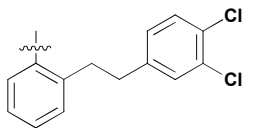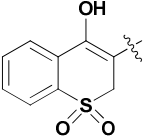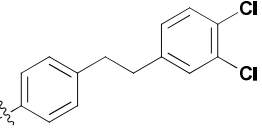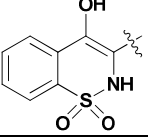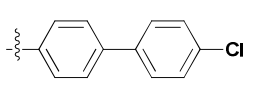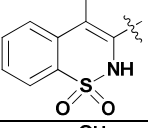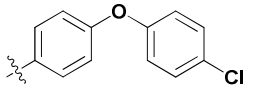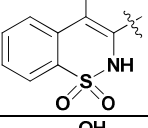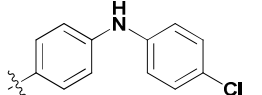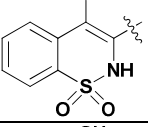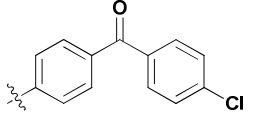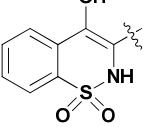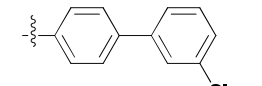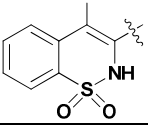
HWB-human whole blood

Table 6: mPGES-1 inhibitory activity of Phenanthrene imidazole derivatives.

Compound	R	mPGES-1 IC$_{50}$ (µM)
57	H	0.251

58	2-Br-Ph	0.506
59	OPh	0.330
60	O(c-hexyl)	0.306
61	OBn	0.172
62	OMe	0.062

Table 7: mPGES-1 inhibitory activity of Imidazoquinoline derivatives.

Compound	R$_1$	R$_2$	Cell free mPGES-1 inhibition	PGE$_2$ inhibition in A549 cells
			IC$_{50}$ (µM)	
64			1.68	3.40
65			0.11	1.14
66			0.29	1.45
67			0.53	6.73
68			0.15	4.24
69			0.11	1.14
70			0.86	3.44
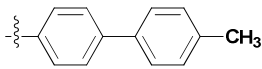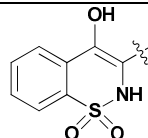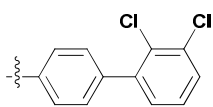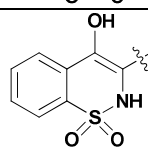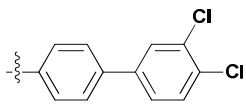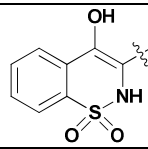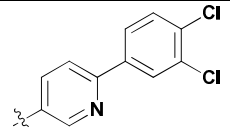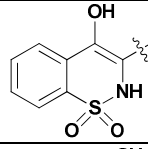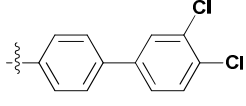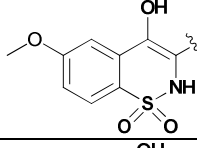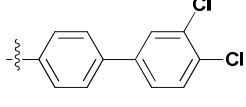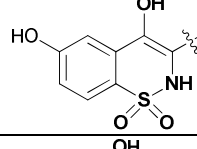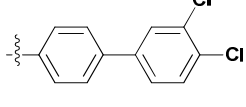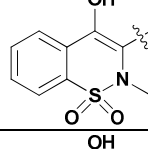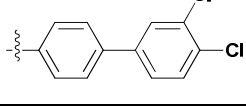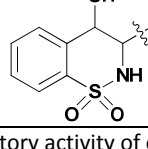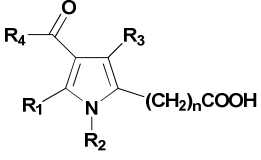
71	(biphenyl-CH₃ structure)	(oxicam OH structure)	<0.07	2.24
72	(dichlorobiphenyl structure)	(oxicam OH structure)	0.038	<0.92
73	(dichlorobiphenyl structure)	(oxicam OH structure)	0.016	0.42
74	(dichlorophenyl pyridine structure)	(oxicam OH structure)	0.16	0.69
75	(dichlorobiphenyl structure)	(methoxy oxicam OH structure)	0.69	1.29
76	(dichlorobiphenyl structure)	(hydroxy oxicam OH structure)	0.098	1.45
77	(dichlorobiphenyl structure)	(N-methyl oxicam OH structure)	0.28	2.04
78	(dichlorobiphenyl structure)	(oxicam OH structure)	0.19	0.67

Table 8: mPGES-1 inhibitory activity of oxicam derivatives.

Compound	R_1	R_2	R_3	R_4	n	Inhibition of mPGES-1 at 1µM (%)
79	CH_3	CH_3	CH_3	$C_{11}H_{23}$	2	54±8
80	CH_3	CH_3	CH_3	$C_{13}H_{27}$	2	91
81	CH_3	CH_3	CH_3	$C_{15}H_{31}$	2	97

82	CH$_3$	CH$_3$	CH$_3$	C$_{11}$H$_{23}$	0	59
83	CH$_3$	CH$_3$	CH$_3$	C$_{11}$H$_{23}$	3	70
84	CH$_3$	Phenyl	CH$_3$	C$_{11}$H$_{23}$	0	99
85	CH$_3$	4-Cl-Benzyl	CH$_3$	C$_{11}$H$_{23}$	2	78
86	CH$_3$	CH$_3$	Phenyl	CH$_3$	2	90
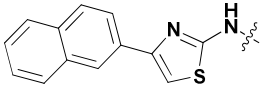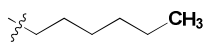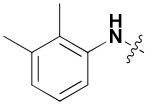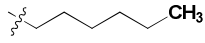
Table 9: mPGES-1 inhibitory activity of Pyrrole alkonic acid derivatives.

Compound	R$_1$	R$_2$	R$_3$	Cell free mPGES-1 inhibition	PGE$_2$ inhibition in A549 cells
				IC$_{50}$ (µM)	
87				n.d.	n.d.
88				1.7	11.9
89				0.008	0.91
90				0.013	3.7
91				0.009	1.8
92				0.012	2.4
93				0.043	2.7

94	(isopropyl–NH–C(=O)–)	(phenyl–C≡C–cyclopropyl)	(–C≡C–phenyl)	0.001	0.16
95	(isopropyl–NH–C(=O)–)	(pyridin-yl–C≡C–Ph)	(–C≡C–phenyl)	0.002	0.36
96	(isopropyl–NH–C(=O)–)	(phenyl–C≡C–pyridin-2-yl)	(–C≡C–C₆H₄–Cl)	0.001	0.48
97	(isopropyl–NH–C(=O)–)	(phenyl–C≡C–pyridin-4-yl)	(–C≡C–C₆H₄–Cl)	0.002	0.34
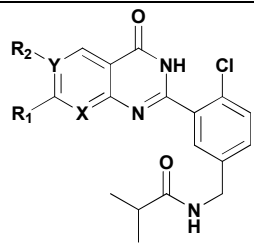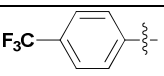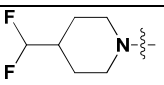
Table 10: mPGES-1 inhibitory activity of Trisubstituted urea derivatives.

$$R_1-\text{pyrimidine}(Cl)-S-CH(R_2)-C(=O)-O-R_3$$
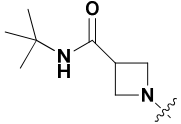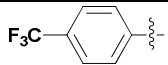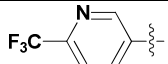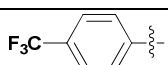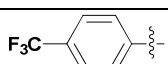
Compound	R_1	R_2	R_3	Cell free mPGES-1 residual activity at 10 µM (% PGE$_2$ of control) (±SEM)	mPGES-1 inhibition	5-LOX inhibition
					IC$_{50}$ (µM)	
98	(2,3-dimethyl-phenyl-NH–)	H_2	H	-	n.i.	n.i.
99	(3,5-bis(CF$_3$CH$_2$O)-phenyl-NH–)	(–(CH$_2$)$_4$CH$_3$)	H	26.7±1.8	2.6	1.5
100	(biphenyl-4-yl-NH–)	(–(CH$_2$)$_4$CH$_3$)	H	21.7±2.9	1.6	0.7
101	(biphenyl-4-yl-CH$_2$-HN–)	(–(CH$_2$)$_4$CH$_3$)	H	21.8±4.2	1.3	1
102	(4'-cyano-biphenyl-4-yl-NH–)	(–(CH$_2$)$_4$CH$_3$)	H	26.1±8.0	1.7	0.4

| 103 | | | H | - | 0.4 | 0.3 |
| 104 | | | H | 40.4±0.05 | 3.4 | - |

n.i. = no inhibition, SEM = Standard Error of Mean
Table 11: mPGES-1 inhibitory activity of pirnixic acid derivatives
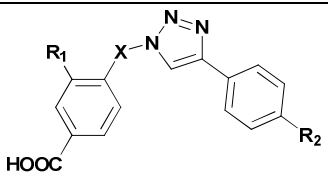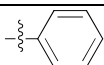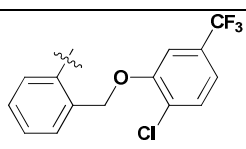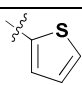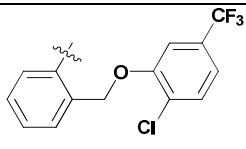
Compound	R$_1$	R$_2$	X	Y	mPGES-1 IC$_{50}$ (µM)(±SEM)	A549 IC$_{50}$ (µM) (±SEM)	HWB IC$_{50}$ (µM) (±SEM)
108	-H	H	C	C	-	-	-
109	-Cl	H	C	C	0.042±0.001	-	-
110	-Br	H	C	C	0.036±0.006	-	-
111	-CF$_3$	H	C	C	0.026±0.002	-	-
112	-cyclopropyl	H	C	C	0.058±0.008	-	-
113	-NO$_2$	H	C	C	0.063±0.010	-	-
114	-OMe	H	C	C	0.304±0.029	-	-
115	Cl		C	C	0.036±0.006	-	-
116	Cl	-cyclopropyl	C	C	0.032±0.007	-	-
117	Cl	-OMe	C	C	0.111±0.014	-	-
118	Cl		C	C	0.024±0.0003	-	-

	R₁	R₂					
119	Cl	(N-tert-butyl azetidine-3-carboxamide)	C	C	0.059±0.005	-	-
120	F₃C–⟨phenyl⟩–	H	C	C	0.007±0.001	0.010±0.001	0.234±0.069
121	F₃C–⟨pyridine⟩–	H	C	C	0.016±0.003	0.023±0.002	-
122	F₃C–⟨phenyl⟩–	H	C	N	0.005±0.001	0.0050±0.0003	0.376±0.093
123	F₃C–⟨phenyl⟩–	H	N	C	0.010±0.001	0.011±0.002	0.328±0.045

SEM = Standard Error of Mean

Table 12: mPGES-1 inhibitory activity of Quinazolin-4(3H)-one derivatives.

Compound	R₁	R₂	X	mPGES-1 IC₅₀ (µM)
123	NO₂	(phenyl)	CH₂	3.2
124	NO₂	(2-((2-chloro-4-(trifluoromethyl)phenoxy)methyl)phenyl)	CH₂	1.2
125	NO₂	(thiophen-2-yl)	CH₂	5.5
126	H	(2-((2-chloro-4-(trifluoromethyl)phenoxy)methyl)phenyl)	CH₂	1
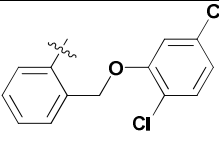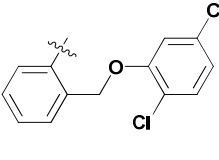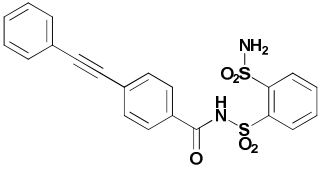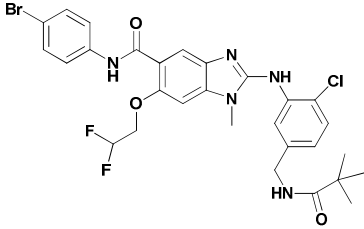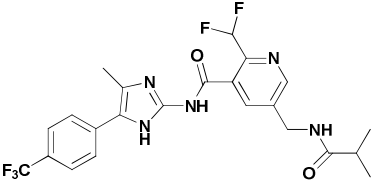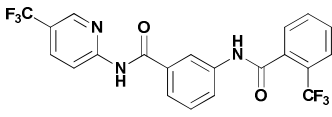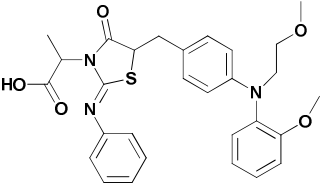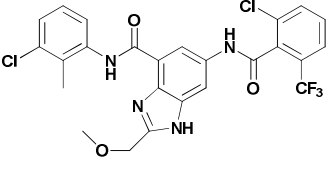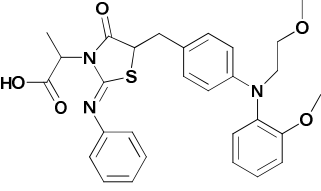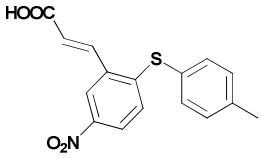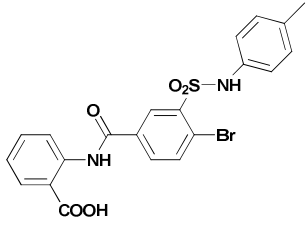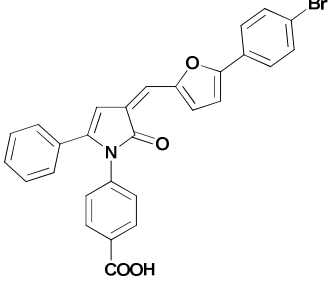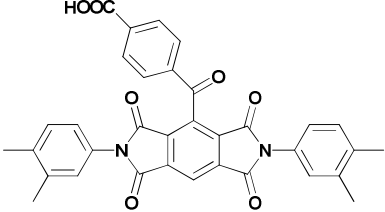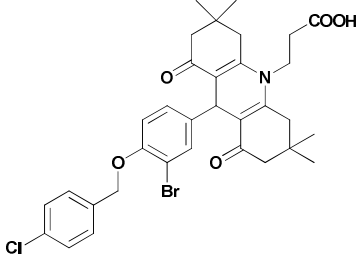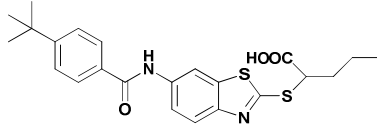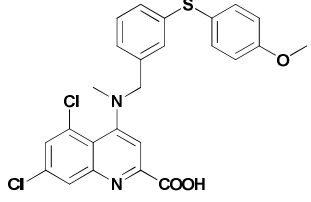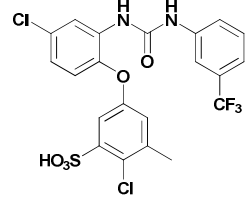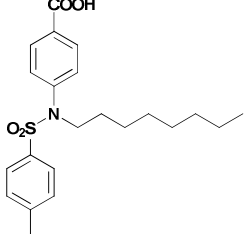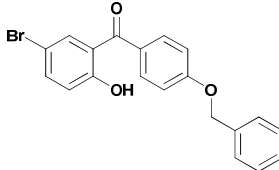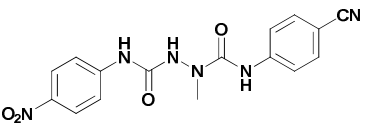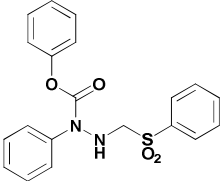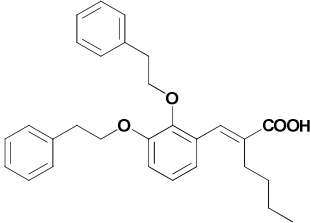
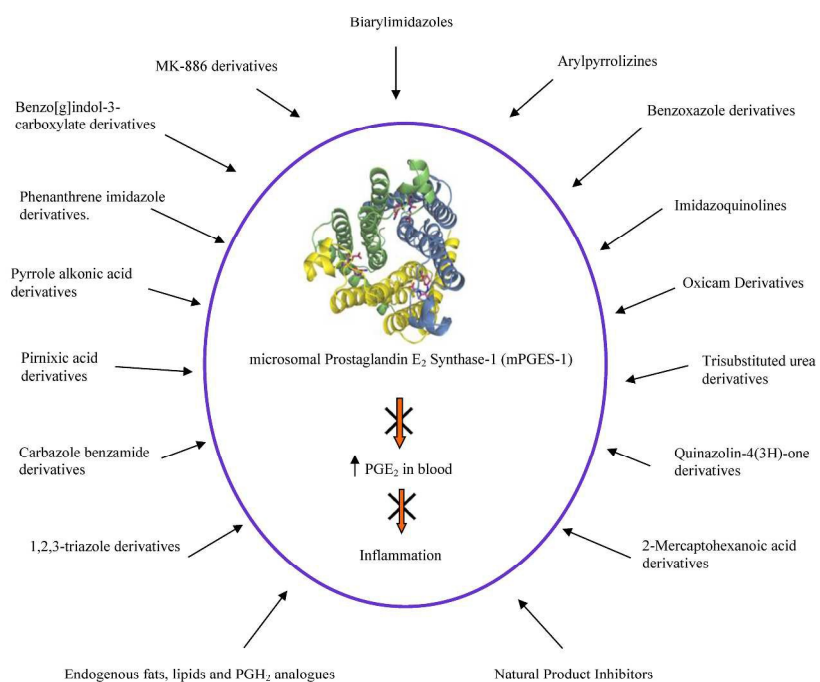| 127 | H | | SO$_2$ | >10 |
| 128 | NH$_2$ | | CH$_2$ | 0.68 |

Table 13: mPGES-1 inhibitory activity of 1,2,3-triazole derivatives.

S.No.	Structure	mPGES-1 IC50(µM)	S.No.	Structure	mPGES-1 IC50(µM)
143		0.010[108]	144		0.003[109]
145		0.00094[110]	146		0.049[111]
147		0.002[112]	148		0.0001[113]
149		0.0035[114]	150		0.0046[114]

151		2.3[115]	152		2.8[115]
153		7.9[115]	154		2.6[115]
155		7.7[115]	156		3.0[115]
157		.40[115]	158		3.7[115]
159		1.4[116]	160		0.9[116]
161		1.7[116]	162		1.1[117]

163		0.0093 ± 0.0005[118]	164		0.0011 ± 0.0001[118]
165		0.0020 ± 0.0002[118]	166		0.0018 ± 0.0001[118]
167		0.0020 ± 0.0001[118]	168		0.0046 ± 0.0001[118]
169		0.0065 ± 0.0002[118]	170		0.0097 ± 0.0008[118]
171		0.0040 ± 0.0002[118]	172		0.10 ± 0.01[118]
173		0.90±0.20[119]	174		5.60±0.40[119]

Table 14: Miscellaneous mPGES-1 inhibitors

279x361mm (300 x 300 DPI)